Thiapentadienyl−Rhodium−Phosphine Chemistry[1]

John R. Bleeke,* Monica Shokeen, and Eric S. Wise

Department of Chemistry, Washington University, One Brookings Drive, St. Louis, Missouri 63130

Nigam P. Rath

Department of Chemistry and Biochemistry, University of Missouri—St. Louis, One University Boulevard, St. Louis, Missouri 63121

Received December 28, 2005

The reactions of $(Cl)Rh(PR_3)_3$ (R = Me, Et) with the anionic thiapentadienide reagent lithium 2,3-dimethyl-5-thiapentadienide have been investigated. Treatment of $(Cl)Rh(PMe_3)_3$ with lithium 2,3-dimethyl-5-thiapentadienide produces ((1,2,5-η)-2,3-dimethyl-5-thiapentadienyl)$Rh(PMe_3)_3$ (**1**), in which the thiapentadienyl ligand is σ-bonded to rhodium through the sulfur end of the chain and π-bonded through the carbon end (C1−C2 double bond). In solution at room temperature, **1** undergoes a rapid dynamic process involving release and recoordination of the thiapentadienyl double bond C1−C2, causing two of the phosphine ligands to become equivalent. The intermediate in which the double bond C1−C2 is released from the rhodium center can be "trapped" as a dioxygen adduct, ((5-η)-2,3-dimethyl-5-thiapentadienyl)-$Rh(PMe_3)_3(\eta^2\text{-}O_2)$ (**2**). When it is stirred at room temperature in tetrahydrofuran solution, **1** slowly rearranges to ((1,4,5-η)-2,3-dimethyl-5-thiapentadienyl)$Rh(PMe_3)_3$ (**3**), the thermodynamic isomer in which the thiapentadienyl ligand is σ-bonded through the carbon end of the chain (C1) and π-bonded through the sulfur end (C4−S double bond). The reactions of both the kinetic and thermodynamic products (**1** and **3**, respectively) with simple electrophiles have been investigated. Treatment of **1** and **3** with $HBF_4 \cdot OEt_2$ results in proton addition to the thiapentadienyl carbon C1 and production of the sulfur-bridged dimer $\{[((2,3,4,5\text{-}\eta)\text{-}2,3\text{-dimethyl-5-thiapentadiene})Rh(PMe_3)_2]_2\}^{2+}(BF_4^-)_2$ (**4**). In contrast, treatment of **1** and **3** with $CH_3O_3SCF_3$ leads to methylation at the nucleophilic sulfur centers and production of $[((1,2,3,4\text{-}\eta)\text{-}2,3,5\text{-trimethyl-5-thiapentadiene})Rh(PMe_3)_3]^+O_3SCF_3^-$ (**5**) and $[((1,4,5\text{-}\eta)\text{-}2,3,5\text{-trimethyl-5-thiapentadienyl})\text{-}Rh(PMe_3)_3]^+O_3SCF_3^-$ (**6**), respectively. When **3** is reacted with methylene chloride (CH_2Cl_2), a double displacement of chlorides by the nucleophilic sulfurs in *two* molecules of **3** leads to a novel methylene-bridged dimer (**7**). Treatment of $(Cl)Rh(PEt_3)_3$ with lithium 2,3-dimethyl-5-thiapentadienide produces ((5-η)-2,3-dimethyl-5-thiapentadienyl)$Rh(PEt_3)_3$ (**8**). Unlike **1**, the terminal carbon−carbon double bond in **8** remains uncoordinated to rhodium due to steric constraints. A sulfur-bridged dimer, $[((5\text{-}\eta)\text{-}2,3\text{-}$dimethyl-5-thiapentadienyl)$Rh(PEt_3)_2]_2$ (**9**), results when **8** is dissolved in acetone at room temperature. The thiapentadienyl bonding mode in **9** is identical with that in **8**, and **9** readily converts back to **8**, upon treatment with PEt_3 in tetrahydrofuran. In *toluene* solution at room temperature, **8** isomerizes to a second sulfur-bridged dimer, $[((1,4,5\text{-}\eta)\text{-}2,3\text{-dimethyl-5-thiapentadienyl})Rh(PEt_3)_2]_2$ (**10**), in which the thiapentadienyl ligand has rearranged to the same mode as observed in **3**. Dimer **10** is produced as a 4:1 mixture of two isomers, a trans isomer (**10a**) possessing inversion symmetry and a cis isomer (**10b**) with C_2 symmetry. The trans isomer **10a** reacts with small ligands, L, to produce mixed dimers of formula $[((1,4,5\text{-}\eta)\text{-}2,3\text{-dimethyl-5-thiapentadienyl})Rh(PEt_3)(L)]_2$ (**12a**, L = PMe_3; **13a**, L = $CNCMe_3$), in which the trans geometry is retained. Compounds **1**−**4**, **7**, **9**, **10a**, **11b** (the $(PMe_3)_4$ analogue of **10b**), **12a**, and **13a** have been characterized by single-crystal X-ray diffraction.

Introduction

During the past two decades, the chemistry of (pentadienyl)-metal complexes has been extensively investigated.[2] Considerably less effort has been directed toward synthesizing and studying the reactivity of (heteropentadienyl)metal complexes,[3] i.e., complexes in which one of the terminal CH_2 groups of the pentadienyl chain has been replaced by a heteroatom such as O, N, P, or S. Like their pentadienyl analogues, these complexes are expected to exhibit a variety of bonding modes and a rich reaction chemistry based on facile ligand rearrangements.

A modest number of thiapentadienyl (or "butadienethiolate") metal complexes have appeared in the literature. Among these are (η^5-1,4-dimethyl-5-thiapentadienyl)$Rh(\eta^5\text{-}C_5H_5)$ (**I**), reported by Angelici,[4] $[(\eta^5\text{-thiapentadienyl})Ru(\eta^6\text{-}C_6Me_6)]^+$ (**II**), synthesized by Rauchfuss,[5] ((1,2,5-η)-5-thiapentadienyl)M(triphos) (**III**; M = Rh, Ir), reported by Bianchini,[6] and a novel ruthenium

(1) Pentadienyl−Metal−Phosphine Chemistry. 33. Part 32: Bleeke, J. R.; Wise, E. S.; Shokeen, M.; Rath, N. P. *Organometallics* **2005**, *24*, 805.

(2) For reviews, see: (a) Ernst, R. D. *Chem. Rev.* **1988**, *88*, 1255. (b) Yasuda, H.; Nakamura, A. *J. Organomet. Chem.* **1985**, *285*, 15. (c) Powell, P. *Adv. Organomet. Chem.* **1986**, *26*, 125. (d) Ernst, R. D. *Comments Inorg. Chem.* **1999**, *21*, 285.

(3) For a recent review of (heteropentadienyl)metal complexes, see: Bleeke, J. R. *Organometallics* **2005**, *24*, 5190.

(4) (a) Spies, G. H.; Angelici, R. J. *Organometallics* **1987**, *6*, 1897. (b) Hachgenei, J. W.; Angelici, R. J. *Angew. Chem., Int. Ed. Engl.* **1987**, *26*, 909. (c) Hachgenei, J. W.; Angelici, R. J. *J. Organomet. Chem.* **1988**, *355*, 359.

10.1021/om058058f CCC: $33.50
Publication on Web 04/11/2006

Chart 1

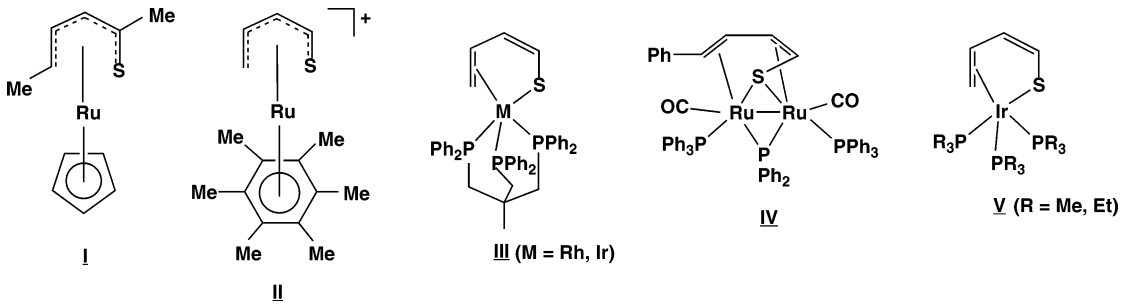

dimer containing the μ_2,η^5-thiapentadienyl ligand, **IV**, obtained recently by Hiraki and Onishi[7] (Chart 1). All of these products were obtained through reactions involving thiophene−metal precursors.

Our group has systematically explored the synthesis of (heteropentadienyl)metal complexes through the use of anionic heteropentadienide reagents and simple halo−transition-metal−phosphine precursors. This approach has led to the production of a large family of oxa-,[8] thia-,[9] aza-,[10] and phosphapentadienyl[11] metal−phosphine complexes. Most closely related to the study at hand are the (thiapentadienyl)iridium complexes ((1,2,5-η)-5-thiapentadienyl)Ir$(PR_3)_3$ (**V**; R = Me, Et),[9] which we obtained earlier from the reactions of (Cl)Ir$(PR_3)_3$ (R = Me, Et) with potassium thiapentadienide. In this paper, we report our recent findings in the analogous (thiapentadienyl)rhodium reaction system; a portion of this work has been previously communicated.[1]

Results and Discussion

A. Synthesis, Spectroscopy, and Structure of (Thiapentadienyl)(trimethylphosphine)rhodium Complexes. As shown in Scheme 1, treatment of (Cl)Rh$(PMe_3)_3$ with the anionic thiapentadienide reagent lithium 2,3-dimethyl-5-thiapentadienide[12] leads to the production of ((1,2,5-η)-2,3-dimethyl-5-thiapentadienyl)Rh$(PMe_3)_3$ (**1**). The η^3 bonding mode of the thiapentadienyl ligand in **1** is evident from the ^{1}H and ^{13}C{^{1}H} NMR spectra. In the ^{1}H NMR, H4 resonates at a typical olefinic value of δ 5.74, while the H1's are shifted substantially upfield to δ 2.53 and 2.21. Similarly, in the ^{13}C{^{1}H} NMR the metal-coordinated carbons, C1 and C2, resonate at δ 43.9 and 73.3, respectively, while the uncoordinated carbons, C3 and C4, appear downfield at δ 139.4 and 121.8, respectively.

Scheme 1

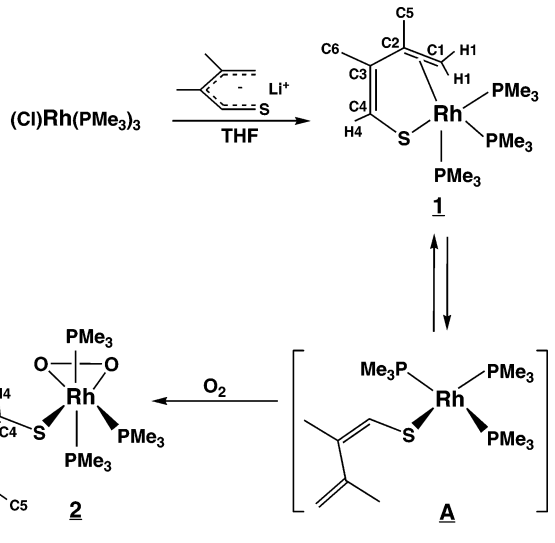

At room temperature, the ^{31}P{^{1}H} NMR spectrum exhibits a deceptively simple pattern consisting of a doublet of triplets (intensity 1) and a doublet of doublets (intensity 2). The large doublet splitting in each case is due to rhodium−phosphorus coupling, while the smaller triplet or doublet splitting is a phosphorus−phosphorus coupling. The simplicity of the pattern results from a rapid solution-phase dynamic process in which the double bond C1−C2 undergoes dissociation from the rhodium center and reassociation (see Scheme 1). The 16e dissociated intermediate (**A**, Scheme 1) possesses mirror-plane symmetry, leading to the observed equivalence of the mutually trans phosphines by NMR. When the temperature is lowered to −70 °C, the dynamic process is slowed, and separate signals for the three inequivalent phosphines are observed. When excess PMe_3 is added to **1** at room temperature, a broad hump is observed in the ^{31}P{^{1}H} NMR, indicating that the added (free) phosphine is exchanging with the coordinated PMe_3 ligands. This phosphine exchange process probably proceeds by addition of PMe_3 to the 16e intermediate **A**, followed by phosphine loss.

The 16e intermediate **A** can be "trapped" irreversibly by exposing compound **1** to air. The resulting peroxo product, ((5-η)-2,3-dimethyl-5-thiapentadienyl)Rh$(PMe_3)_3(\eta^2$-$O_2)$ (**2**; Scheme 1), exhibits ^{1}H and ^{13}C NMR signals that are *all* in the downfield (uncoordinated) region, indicating the presence of an S-bound η^1-thiapentadienyl ligand. In particular, H4 resonates at δ 6.51, the H1's resonate at δ 5.12 and 4.83, and the four thiapentadienyl chain carbons resonate between δ 111.7 and 146.2. The ^{31}P{^{1}H} NMR spectrum is consistent with an octahedral

(5) (a) Luo, S.; Rauchfuss, T. B.; Wilson, S. R. *J. Am. Chem. Soc.* **1992**, *114*, 8515. (b) Luo, S.; Rauchfuss, T. B.; Gan, Z. *J. Am. Chem. Soc.* **1993**, *115*, 4943.

(6) (a) Bianchini, C.; Meli, A.; Peruzzini, M.; Vizza, F.; Frediani, P.; Herrera, V.; Sanchez-Delgado, R. A. *J. Am. Chem. Soc.* **1993**, *115*, 2731. (b) Bianchini, C.; Jimenez, M. V.; Meli, A.; Vizza, F. *Organometallics* **1995**, *14*, 3196. (c) Bianchini, C.; Frediani, P.; Herrera, V.; Jimenez, M. V.; Meli, A.; Rincon, L.; Sanchez-Delgado, R.; Vizza, F. *J. Am. Chem. Soc.* **1995**, *117*, 4333. (d) Bianchini, C.; Jimenez, M. V.; Meli, A.; Moneti, S.; Vizza, F. *J. Organomet. Chem.* **1995**, *504*, 27.

(7) Kawano, H.; Narimatsu, H.; Yamamoto, D.; Tanaka, K.; Hiraki, K.; Onishi, M. *Organometallics* **2002**, *21*, 5526.

(8) (a) Bleeke, J. R.; Haile, T.; Chiang, M. Y. *Organometallics* **1991**, *10*, 19. (b) Bleeke, J. R.; Haile, T.; New, P. R.; Chiang, M. Y. *Organometallics* **1993**, *12*, 517. (c) Bleeke, J. R.; New, P. R.; Blanchard, J. M. B.; Haile, T.; Beatty, A. M. *Organometallics* **1995**, *14*, 5127. (d) Bleeke, J. R.; Donnay, E.; Rath, N. P. *Organometallics* **2002**, *21*, 4099.

(9) (a) Bleeke, J. R.; Ortwerth, M. F.; Chiang, M. Y. *Organometallics* **1992**, *11*, 2740. (b) Bleeke, J. R.; Ortwerth, M. F.; Rohde, A. M. *Organometallics* **1995**, *14*, 2813.

(10) Bleeke, J. R.; Luaders, S. T.; Robinson, K. D. *Organometallics* **1994**, *13*, 1592.

(11) (a) Bleeke, J. R.; Rohde, A. M.; Robinson, K. *Organometallics* **1994**, *13*, 401. (b) Bleeke, J. R.; Rohde, A. M.; Robinson, K. D. *Organometallics* **1995**, *14*, 1674.

(12) (a) Bleeke, J. R.; Hinkle, P. V.; Rath, N. P. *J. Am. Chem. Soc.* **1999**, *121*, 595. (b) Bleeke, J. R.; Hinkle, P. V.; Rath, N. P. *Organometallics* **2001**, *20*, 1939.

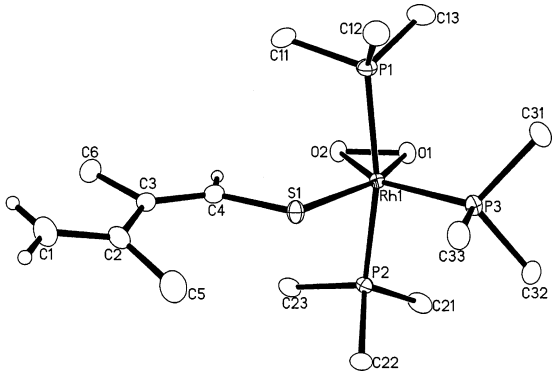

Figure 1. ORTEP drawing of **2**, using thermal ellipsoids at the 50% level. Methyl H's are not shown. Selected bond distances (Å): Rh1−P1, 2.3190(4); Rh1−P2, 2.3157 (4); Rh1−P3, 2.2833-(4); Rh1−S1, 2.3904(4); Rh1−O1, 2.0269(10); Rh1−O2, 2.0579-(10); O1−O2, 1.4496(14); C1−C2, 1.339(2); C2−C3, 1.473(2); C3−C4, 1.354(2); C4−S1, 1.7450 (15).

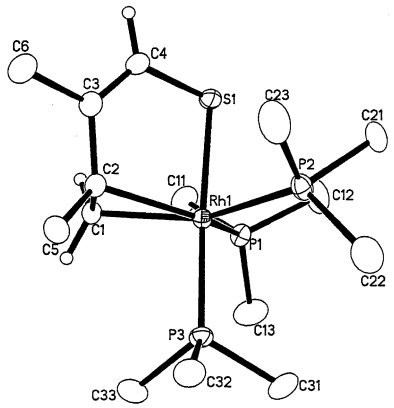

Figure 2. ORTEP drawing of **1**, using thermal ellipsoids at the 30% level. Methyl H's are not shown. Selected bond distances (Å): Rh1−P1, 2.3512(7); Rh1−P2, 2.3385(7); Rh1−P3, 2.2668-(7); Rh1−S1, 2.3992(7); Rh1−C1, 2.137(2); Rh1−C2, 2.222(2); C1−C2, 1.437(4); C2−C3, 1.505(4); C3−C4, 1.339(4); C4−S1, 1.741(3).

coordination geometry in which the three PMe_3 ligands are oriented in a *mer* arrangement.

The structure of **2** has been confirmed by single-crystal X-ray diffraction and is presented in Figure 1. As expected, the peroxo ligand lies in the molecule's equatorial plane and is situated trans to the S-bound η^1-thiapentadienyl ligand and to one of the phosphine ligands (P3). The other phosphines (P1 and P2) lie trans to one another. Thiapentadienyl atoms C2, C3, C4, and S1 are essentially coplanar (mean deviation 0.016 Å), but rotation about the single bond C2−C3 causes C1 to lie 0.29 Å out of that plane. Overall, the thiapentadienyl ligand adopts a sickle shape with torsional angles of 167.6(1)° for C1−C2−C3−C4 and −5.9(2)° for C2−C3−C4−S1.[13] Thiapentadienyl carbon−carbon bond distances alternate in the expected way with C1−C2 = 1.339(2) Å, C2−C3 = 1.473(2) Å, and C3−C4 = 1.354(2) Å.

The X-ray crystal structure of compound **1** has also been obtained and is presented in Figure 2.[14] The coordination geometry about rhodium is a distorted octahedron with the three phosphines situated in a *fac* arrangement and C1, C2, and S1 occupying the three remaining sites. Rh1, C2, C3, C4, and S1 are roughly coplanar (mean deviation 0.0864 Å), while C1 resides out of this plane by 1.39 Å. As expected, the C1−C2 distance has lengthened to 1.437(4) Å as a result of π-back-bonding, while the C2−C3 and C3−C4 bond lengths are typical for C−C single and double bonds, respectively. Phosphorus atom P3, which is situated trans to S1, displays a significantly shorter bond to rhodium than do P1 and P2, which reside opposite carbon atoms.

When compound **1** is stirred in tetrahydrofuran for 48 h, it gradually isomerizes to ((1,4,5-η)-2,3-dimethyl-5-thiapentadienyl)$Rh(PMe_3)_3$ (**3**; Scheme 2), in which the thiapentadienyl ligand is σ-bonded to rhodium through the carbon end of the chain (C1) and π-bonded through the sulfur end (C4−S double bond).[15] As before, the ^1H and $^{13}C\{^1H\}$ NMR spectra of **3** are diagnostic. In the ^1H NMR, the signal for H4 is shifted upfield to δ 4.09 (from its position at δ 5.74 in **1**), while the H1's are likewise upfield-shifted to δ 2.25 and 1.10 (from δ 2.53 and 2.21 in **1**). In the $^{13}C\{^1H\}$ spectra, the π-coordinated carbon C4 resonates at δ 73.6 (vs δ 121.8 in **1**), while the σ-coordinated carbon C1 appears at δ 32.2 and is strongly coupled to a trans PMe_3 ligand (J_{C-P} = 98.8 Hz). Uncoordinated carbons C2 and C3 resonate at δ 142.0 and 136.0. Unlike **1**, compound **3** is not fluxional at room temperature and gives rise to three well-separated doublet-of-doublet-of-doublets patterns in the $^{31}P\{^1H\}$ NMR. For each signal, the largest splitting is due to rhodium−phosphorus coupling, while the smaller splittings are phosphorus−phosphorus couplings. Interestingly, the rhodium−phosphorus coupling constants vary widely and provide a rough measure of phosphine lability (vide infra). The phosphine that lies trans to sulfur exhibits the largest J_{Rh-P} value (162.9 Hz), while the phosphines trans to C4 and C1 have J_{Rh-P} values of 123.4 and 80.0 Hz, respectively. In the presence of excess PMe_3, the conversion of **1** to **3** is completely shut down, strongly implying that a PMe_3 dissociation is required. This, in turn, suggests that an η^5-thiapentadienyl species (**B**; Scheme 2) may serve as a key intermediate.

Compound **3** is the first example of a thiapentadienyl−metal complex containing a 5-thiapentadienyl ligand in the 1,4,5-η bonding mode. It is interesting that this bonding mode has not been previously observed in the closely analogous iridium system or in related rhodium systems. For example, we showed earlier that ((1,2,5-η)-5-thiapentadienyl)$Ir(PMe_3)_3$ (**V** in Chart 1) is stable indefinitely at room temperature.[9] Even when **V** is heated in toluene at reflux, we saw no evidence for thiapentadienyl ligand isomerization; rather, C−H2 bond activation occurred, leading to the production of an iridathiacyclopentene complex.[9b] This absence of thiapentadienyl ligand isomerization

(13) There is one previous X-ray structure of an η^1-thiapentadienyl−metal complex, and it too exhibits the sickle-shaped geometry for the thiapentadienyl ligand.[4c]

(14) The structure bears a strong resemblance to that of ((1,2,5-η)-5-thiapentadienyl)$Ir(PMe_3)_3$, which we reported earlier.[9a]

(15) The coordination of the C4−S double bond to rhodium results in the formation of a thioaldehyde−metal complex. Thioaldehyde−metal complexes are not uncommon in organometallic chemistry, and examples involving early, middle, and late transition metals have been reported. However, it appears that the compounds reported herein are the first examples of η^2-thioaldehyde−rhodium complexes that have been structurally characterized by X-ray diffraction. Leading references: (a) Collins, T. J.; Roper, W. R. *J. Organomet. Chem.* **1978**, *159*, 73. (b) Hill, A. F.; Roper, W. R.; Waters, J. M.; Wright, A. H. *J. Am. Chem. Soc.* **1983**, *105*, 5940. (c) Buhro, W. E.; Patton, A. T.; Strouse, C. E.; Gladysz, J. A.; McCormick, F. B.; Etter, M. C. *J. Am. Chem. Soc.* **1983**, *105*, 1056. (d) Werner, H.; Hofmann, L.; Wolf, J.; Muller, G. *J. Organomet. Chem.* **1985**, *280*, C55. (e) Mayr, A.; McDermott, G. A.; Dorries, A. M.; Holder, A. K.; Fultz, W. C.; Rheingold, A. L. *J. Am. Chem. Soc.* **1986**, *108*, 310. (f) Buchwald, S. L.; Nielson, R. B.; Dewan, J. C. *J. Am. Chem. Soc.* **1987**, *109*, 1590. (g) Fischer, H. *J. Organomet. Chem.* **1988**, *345*, 65. (h) Werner, H.; Paul, W.; Knaup, W.; Wolf, J.; Muller, G.; Riede, J. *J. Organomet. Chem.* **1988**, *358*, 95. (i) Werner, H.; Steinmetz, M.; Peters, K.; von Schnering, H. G. *Eur. J. Inorg. Chem.* **1998**, 1605. (j) Burzlaff, N.; Schenk, W. A. *Eur. J. Inorg. Chem.* **1999**, 1435.

Scheme 2

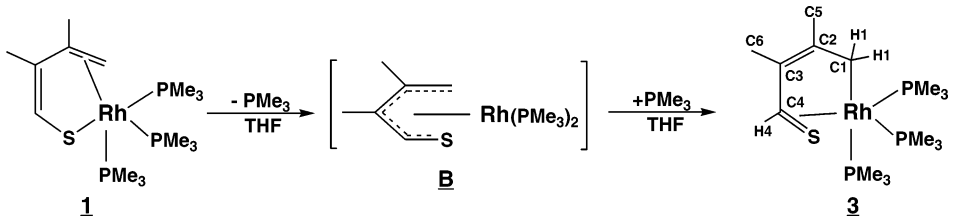

in the iridium system may reflect stronger Ir−PMe_3 bonds (versus Rh−PMe_3) and hence the inaccessibility of the key η^5-thiapentadienyl intermediate (cf. **B**; Scheme 2). Similarly, Bianchini's close relative of **1**, ((1,2,5-η)-5-thiapentadienyl)-Rh(triphos) (**III** in Chart 1), did not undergo isomerization to the 1,4,5-η-5-thiapentadienyl bonding mode.[6b,c] A likely explanation in this case is that the strongly chelating nature of the triphos ligand prevented phosphine loss and formation of the η^5-thiapentadienyl intermediate.

The X-ray crystal structure of **3** has been obtained and is presented in Figure 3. The coordination geometry is distorted octahedral with the phosphines adopting a *fac* arrangement and C1, C4, and S1 occupying the remaining coordination sites. The rhodium atom and the four thiapentadienyl chain carbons are roughly coplanar (mean deviation 0.103 Å) and together form a metallacyclopentene, while S1 resides 1.76 Å out of this plane. The carbon−carbon bonds within the metallacycle exhibit the expected alternation in bond lengths. The phosphine that lies trans to S1 (P3) exhibits a significantly shorter Rh−P bond than the other two phosphines (P1 and P2), consistent with the Rh−P coupling constants discussed above.

The reason for the stability of the (1,4,5-η)-5-thiapentadienyl bonding mode in **3** vs the 1,2,5-η bonding mode in **1** is not entirely clear. It may be that the C═S group is a better π-acceptor than C═C. This is suggested by the very long C−S bond length of 1.777(4) Å in **3** (a typical C−S single bond is 1.82 Å).[16] In addition, the Rh−S1−C4 interaction, which can be viewed as a metallathiacyclopropane, may be significantly less strained that the Rh−C1−C2 metallacyclopropane in **1**. This reduced ring strain would, in turn, result from sulfur's ability to use essentially unhybridized p orbitals to bond with carbon and rhodium.[17] Further evidence for the greater strength of the Rh1−S1−C4 interaction in **3** versus the Rh1−C1−C2 interaction in **1** is the fact that the double bond S1−C4 does *not* reversibly dissociate from the Rh center in compound **3**, while the double bond C1−C2 does dissociate in compound **1** (vide supra).

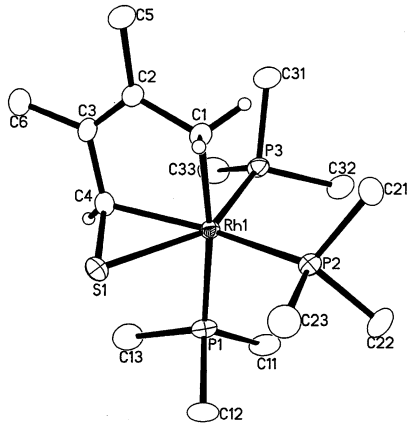

Figure 3. ORTEP drawing of **3**, using thermal ellipsoids at the 30% level. Methyl H's are not shown. There are two independent molecules in the unit cell; molecule 1 is shown here. Selected bond distances (Å): Rh1−P1, 2.3478(11); Rh1−P2, 2.3254(10); Rh1−P3, 2.2710(10); Rh1−S1, 2.3927(9); Rh1−C1, 2.123(4); Rh1−C4, 2.097(4); C1−C2, 1.500(5); C2−C3, 1.327(5); C3−C4, 1.487(5); C4−S1, 1.777(4).

B. Reaction Chemistry of (Thiapentadienyl)(trimethylphosphine)rhodium Complexes. 1. Reactivity of the Kinetic Isomer. The reactivity of the kinetic isomer ((1,2,5-η)-2,3-dimethyl-5-thiapentadienyl)Rh(PMe_3)$_3$ (**1**) toward simple electrophiles has been investigated. As shown in Scheme 3, treatment of **1** with HBF_4·OEt_2 leads to the production of the sulfur-bridged dimer {[((2,3,4,5-η)-2,3-dimethyl-5-thiapentadiene)-Rh(PMe_3)$_2$]$_2$}$^{2+}$(BF_4^-)$_2$ (**4**).[18] While the detailed mechanism of this reaction is not known, it seems likely that the initial site of H^+ attack is the electron-rich metal center (see **C**; Scheme 3). The resulting metal hydride can then migrate to C1 of the thiapentadienyl group, converting it to the observed thiapentadiene ligand. Phosphine loss, followed by dimerization through sulfur bridges, completes the reaction.

The NMR spectra of **4** are consistent with its formulation as a ((2,3,4,5-η)-5-thiapentadiene)Rh complex. In particular, the ^{13}C NMR signals for carbons C3 and C4 (which are now π-coordinated) are upfield-shifted to δ 125.3 and 104.3, respectively, from their positions of δ 139.4 and 121.8 in the starting material **1**. Carbon C2 resonates at δ 62.9, while C1 (which is now a methyl carbon) resonates at δ 29.0. In the ^{1}H NMR, the signal for H4 appears at δ 7.05, while the methyl protons on C1 resonate at δ 1.20. The downfield chemical shift position for H4 is surprising and may reflect the presence of some thioaldehyde character in **4**. The ^{31}P{^{1}H} NMR consists of essentially two doublet-of-doublet signals for the two inequivalent phosphines. In each case, the larger doublet is due to Rh−P coupling, while the smaller doublet results from P−P coupling. The signals show some second-order effects, which result from long-range couplings between the halves of the dimer.

The structure of **4** has been confirmed by X-ray diffraction and is presented in Figure 4. The molecule sits on a crystallographically imposed inversion center, which relates the halves of the molecule by symmetry. The pseudo-octahedral coordination environment around the rhodium atom is highly distorted, but one of the phosphines (P1) lies approximately trans to the thiapentadiene sulfur (S1) (the angle P1−Rh1−S1 is 153.96-(7)°), while the other phosphine (P2) lies approximately trans to thiapentadiene carbon C4 (the angle P2−Rh1−C4 is 148.9-(2)°). The thiapentadiene carbon C2 lies approximately trans to the bridging sulfur S1′ (the angle S1′−Rh1−C2 is 159.5-(2)°). The bond distances within the coordinated thiapentadiene moiety reflect the expected delocalization. Hence, bonds C2−

(16) Huheey, J. E. *Inorganic Chemistry: Principles of Structure and Reactivity*; Harper & Row: New York, 1972; Appendix F and references therein.

(17) Huheey, J. E. *Inorganic Chemistry: Principles of Structure and Reactivity*; Harper & Row: New York, 1972; pp 130−133.

(18) Treatment of **4** with base in the presence of PMe_3 does not regenerate **1**.

Scheme 3

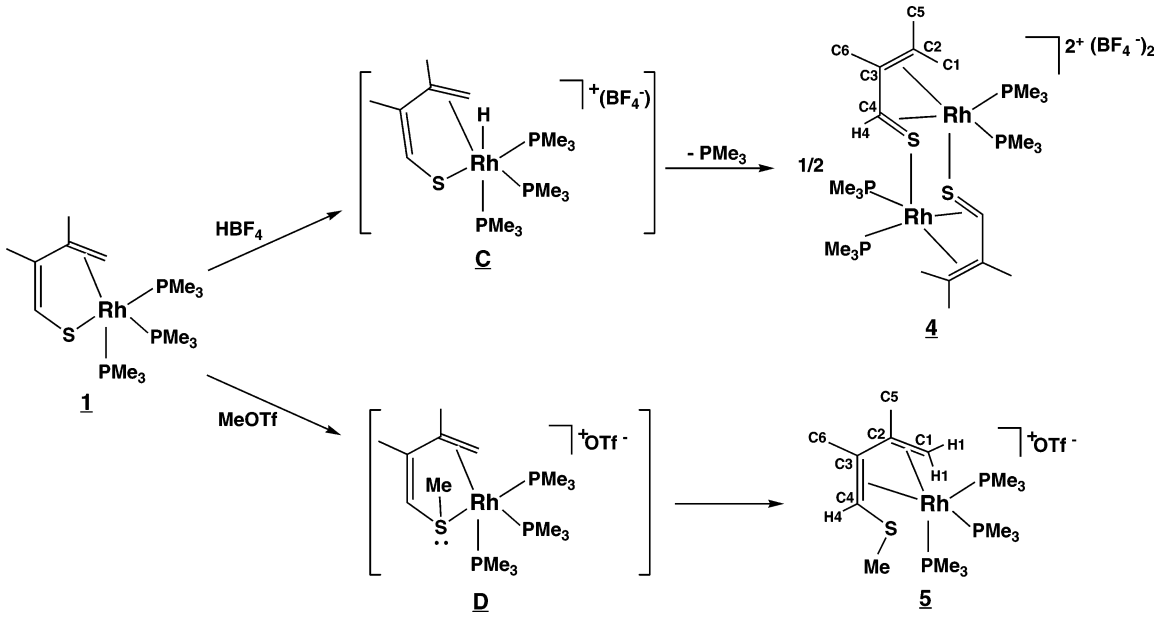

C3 (1.430(11) Å), C3−C4 (1.469(12) Å), and C4−S1 (1.747(8) Å) all display distances that are intermediate between single- and double-bond lengths.

When compound **1** is treated with the electrophilic reagent methyl triflate (MeO_3SCF_3), methylation occurs at the electron-rich sulfur center, leading ultimately to the production of [((1,2,3,4-η)-2,3,5-trimethyl-5-thiapentadiene)$Rh(PMe_3)_3]^+O_3SCF_3^-$ (**5**; Scheme 3). The likely intermediate, **D** in Scheme 3, cannot be isolated under our reaction conditions.

In the $^{13}C\{^1H\}$ NMR spectrum of **5**, the carbons of the diene chain resonate at δ 116.0 (C2), 101.8 (C3), 55.1 (C4), and 47.1 (C1), all within the expected range for π-coordinated carbons. C4 and C1 exhibit significant carbon−phosphorus coupling constants of 57.6 and 34.7 Hz, respectively. The *S*-methyl peak is observed at δ 21.0. In the ^1H NMR spectrum, H4 resonates at δ 3.42, while the two H1 protons resonate at δ 2.67 and 2.37. The *S*-Me signal appears at δ 2.11, close to the position of the other two methyl groups on the thiapentadiene chain. As expected, the $^{31}P\{^1H\}$ NMR spectrum exhibits three well-separated doublet-of-doublet-of-doublets patterns with large rhodium−phosphorus couplings and much smaller phosphorus−phosphorus couplings.

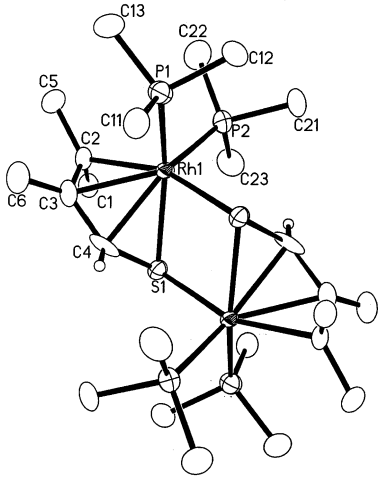

Figure 4. ORTEP drawing of the dication in **4**, using thermal ellipsoids at the 50% level. Methyl H's are not shown. Selected bond distances (Å): Rh1−P1, 2.299(2); Rh1−P2, 2.295(2); Rh1−S1, 2.4325(19); Rh1−S1′, 2.4240(18); Rh1−C2, 2.243(7); Rh1−C3, 2.247(7); Rh1−C4, 2.191(7); C1−C2, 1.547(12); C2−C3, 1.430(11); C3−C4, 1.469(12); C4−S1, 1.747(8).

The reactivity of **1** toward electrophiles is very similar to that observed earlier for ((1,2,5-η)-5-thiapentadienyl)$Ir(PMe_3)_3$.[9b] In that system, H^+ added to C1 to produce [((2,3,4,5-η)-5-thiapentadiene)$Ir(PMe_3)_3]^+$, but this species remained monomeric rather than dimerizing through sulfur bridges. The failure to dimerize may simply reflect a stronger M−PMe_3 interaction in the Ir system versus that in the Rh system. Me^+ attacked the sulfur center in ((1,2,5-η)-5-thiapentadienyl)$Ir(PMe_3)_3$, ultimately generating an iridium analogue of **5**.[9b] Bianchini observed a similar reactivity pattern for ((1,2,5-η)-5-thiapentadienyl)Rh(triphos) (**III**; Chart 1).[6c] Hence, H^+ added to C1 while Me^+ attacked sulfur. The protonation product remained monomeric, probably due to the strong chelating nature of the triphos ligand. The methylation product retained the (1,2,5-η)-5-thiapentadiene bonding mode, rather than rearranging to the 1,2,3,4-η mode.

2. Reactivity of the Thermodynamic Isomer. As shown in Scheme 4, treatment of the thermodynamic isomer ((1,4,5-η)-2,3-dimethyl-5-thiapentadienyl)$Rh(PMe)_3$ (**3**) with $HBF_4{\cdot}OEt_2$ leads to compound **4**, the same product as was obtained in the reaction of kinetic isomer **1** with $HBF_4{\cdot}OEt_2$ (vide supra). Again, it seems likely that the initial site of H^+ attack is the electron-rich metal center. Rapid reductive elimination of the resulting metal hydride with C1 of the thiapentadienyl group would convert it to the observed thiapentadiene ligand.

When compound **3** is treated with methyl triflate, methylation again occurs at the nucleophilic sulfur center, producing [((1,4,5-η)-2,3,5-trimethyl-5-thiapentadienyl)$Rh(PMe_3)_3]^+O_3SCF_3^-$ (**6**; see Scheme 4). The sulfur atom in **3** possesses *two* lone pairs, either of which could be the site of attack, but a preliminary X-ray crystal structure of **6**[19] shows that the methyl group selectively attacks the lone pair that points up toward the

(19) Crystal data for **6**·(acetone): formula $C_{20}H_{45}F_3O_4P_3RhS_2$; fw = 666.50; monoclinic, space group $P2_1/c$; a = 16.0448(9) Å, b = 11.4484(6) Å, c = 16.7728(9) Å, β = 107.102(3)°, V = 2944.7(3) Å^3; Z = 4; d_{calcd} = 1.503 g/cm^3.

Scheme 4

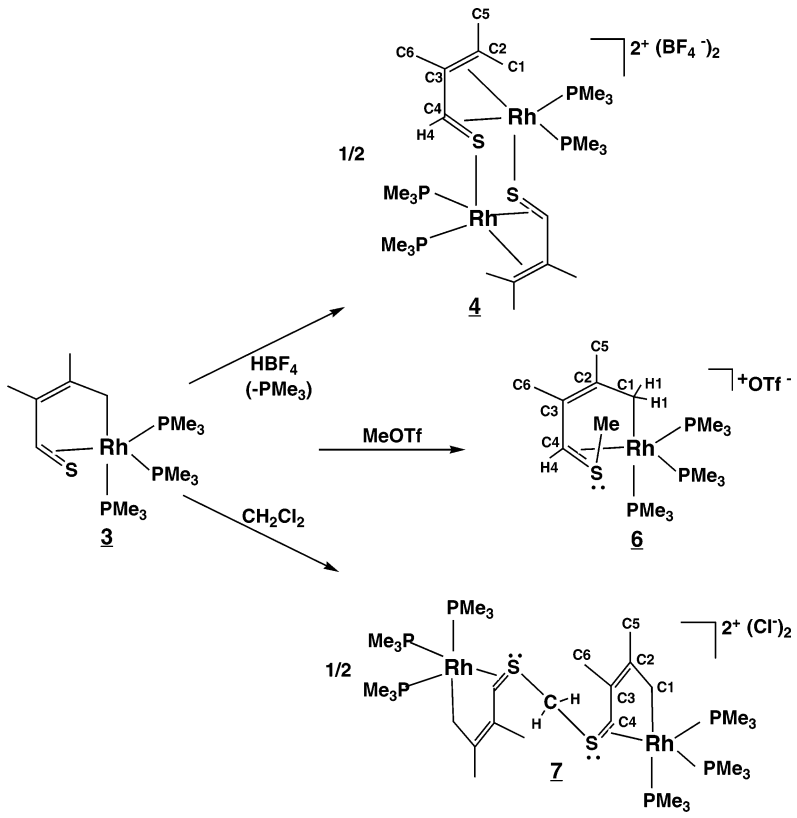

thiapentadienyl ligand (as shown in Scheme 4), rather than the lone pair that faces down toward the bulky axial phosphine.

The NMR data for **6** are very similar to those of starting material **3**. In the ^{1}H NMR, H4 resonates at δ 3.83 (vs δ 4.09 in **3**), while the H1's appear at δ 1.75 and 1.55 (vs δ 2.25 and 1.10 in **3**). The *S*-methyl group is observed at δ 1.63. In the ^{13}C{^{1}H} NMR, π-coordinated carbon C4 resonates at δ 64.7 (vs δ 73.6 in **3**) and couples to phosphorus with $J_{C-P} = 57.5$ Hz, while the σ-coordinated carbon C1 appears at δ 36.7 (vs δ 32.2 in **3**) and couples to phosphorus with $J_{C-P} = 76.5$ Hz. The uncoordinated carbons C2 and C3 resonate at δ 149.4 and 134.5 (vs δ 142.0 and 136.0 in **3**). The *S*-methyl resonance is the most upfield peak in the ^{13}C{^{1}H} NMR spectrum, appearing at δ 10.1. The ^{31}P{^{1}H} NMR spectrum of **6** also closely resembles that of **3**, in that there are three well-separated signals, each of which exhibits rhodium and phosphorus coupling. As in the spectrum of **3**, the three Rh−P coupling constants differ quite markedly. The phosphine trans to sulfur exhibits the largest J_{Rh-P} value (161.7 Hz), while the phosphines trans to C4 and C1 have rhodium couplings of 112.9 and 77.8 Hz, respectively.

When compound **3** is dissolved in methylene chloride (CH_2Cl_2), a double displacement of chlorides by the nucleophilic sulfur centers in *two* molecules of **3** leads to the production of a novel methylene-bridged dimer, **7** (see Scheme 4). The NMR data for **7** bear a strong resemblance to those of **6**, except that new peaks for the bridging CH_2 group appear at δ 2.22 in the ^{1}H NMR spectrum and at δ 24.4 in the ^{13}C{^{1}H} NMR spectrum, replacing the *S*-methyl resonances in **6**. The X-ray crystal structure of **7** has been obtained and is presented in Figure 5. The molecule exhibits a 2-fold disorder (not shown in Figure 5), which allows the bridging methylene carbon (C7) to serve as a crystallographic inversion center. As expected, the bridging methylene group projects toward the thiapentadienyl ligand rather than in the opposite direction, where it would encounter steric interactions with phosphine P1.

C. Synthesis, Spectroscopy, and Structure of (Thiapentadienyl)(triethylphosphine)rhodium Complexes. When (Cl)Rh(PEt$_3$)$_3$ is treated with lithium 2,3-dimethyl-5-thiapentadienide,[12] the product is an η^1-thiapentadienyl species, ((5-η)-2,3-dimethyl-5-thiapentadienyl)Rh(PEt$_3$)$_3$ (**8**; Scheme 5). The increased steric bulk of the PEt$_3$ ligands is apparently responsible for the 16e η^1 ground-state structure. Furthermore, structural evidence presented below strongly implies that the η^1-thiapentadienyl ligand in **8** possesses a trans internal double bond (C3−C4), in contrast to the cis internal double bond in **1** and in the

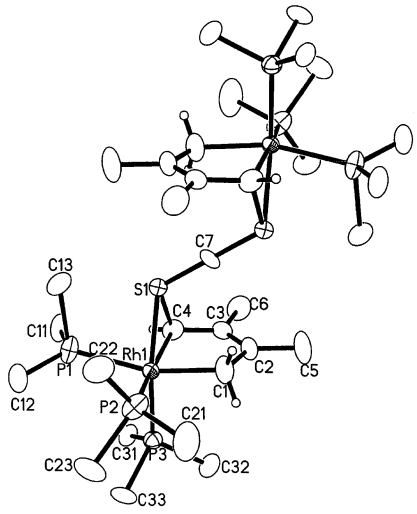

Figure 5. ORTEP drawing of the dication in **7**, using thermal ellipsoids at the 50% level. Methyl H's and the H's on the bridging methylene (C7) are not shown. Selected bond distances (Å): Rh1−P1, 2.3667(13); Rh1−P2, 2.3632(14); Rh1−P3, 2.2750(12); Rh1−S1, 2.334(2); Rh1−C1, 2.098(5); Rh1−C4, 2.092(4); C1−C2, 1.492(7); C2−C3, 1.334(7); C3−C4, 1.482(7); C4−S1, 1.924(5); S1−C7, 1.797(2).

Scheme 5

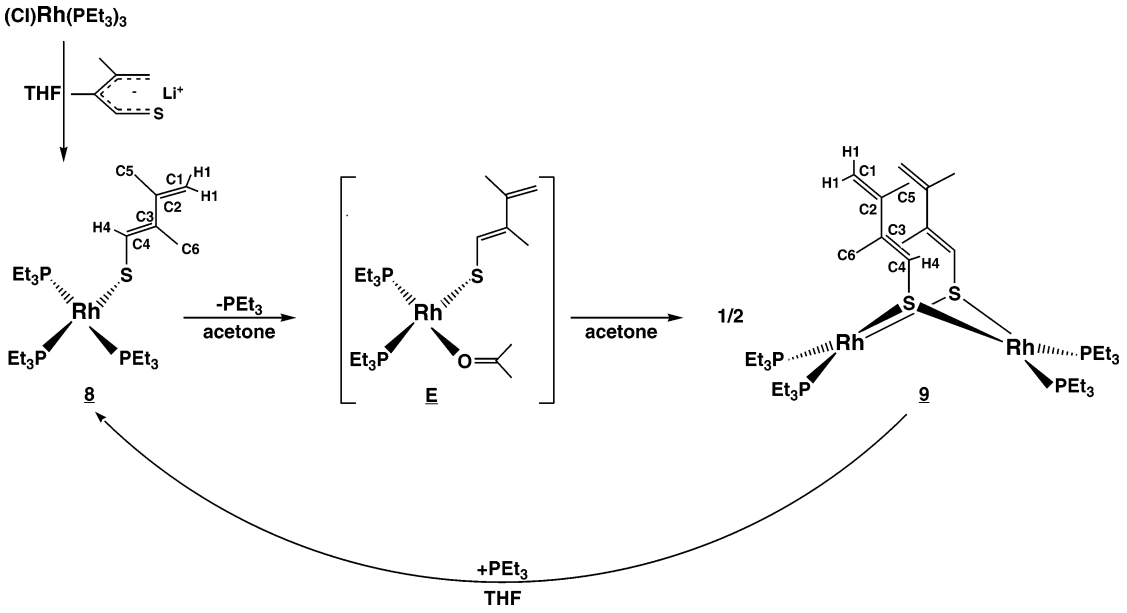

lithium thiapentadienide starting material. This rearrangement, which probably proceeds through a transient C3-bound (η^1-thiapentadienyl)rhodium intermediate, minimizes steric contacts between the thiapentadienyl chain and the PEt_3 ligands.

In the ^1H and $^{13}C\{^1H\}$ NMR spectra of **8**, all of the thiapentadienyl signals appear in the downfield (uncoordinated) region. H4 resonates at δ 7.22, while the two H1's resonate at δ 4.95 and 4.80; the thiapentadienyl carbons appear at δ 144.5 (C2), 137.7 (C4), 130.1 (C3), and 105.0 (C1). The $^{31}P\{^1H\}$ NMR spectrum consists of just two signals, a doublet of doublets (intensity 2) and a doublet of triplets (intensity 1), consistent with a square-planar complex possessing mirror plane symmetry. The spectrum does not change upon cooling to −70 °C.

When ((5-η)-2,3-dimethyl-5-thiapentadienyl)$Rh(PEt_3)_3$ (**8**) is stirred in acetone, a dimeric product containing S-bound η^1-thiapentadienyl ligands can be isolated (**9**; Scheme 5). The coordinating solvent (acetone) is key to this reaction, because it can trap "(η^1-thiapentadienyl)$Rh(PEt_3)_2$" as an acetone adduct (**E**; Scheme 5) as soon as it is formed by PEt_3 dissociation from **8**. This trapping, in turn, prevents coordination of the thiapentadienyl double bonds, a process which ultimately leads to a *different* dimeric product (vide infra).

The ^1H and $^{13}C\{^1H\}$ NMR spectra of **9** are diagnostic for the S-bound η^1-thiapentadienyl bonding mode and bear a close resemblance to those of **8**. In particular, the thiapentadienyl protons resonate downfield at δ 6.96 (H4), 4.74 (H1), and 4.66 (H1), while the thiapentadienyl carbons resonate at δ 146.2 (C2), 134.7 (C3), 133.7 (C4), and 107.8 (C1). Because all four PEt_3 ligands are chemically equivalent, the $^{31}P\{^1H\}$ NMR signal is a simple rhodium-coupled doublet.

The structure of **9** has been confirmed by X-ray diffraction and is presented in Figure 6. The Rh_2S_2 core of **9** is bent with Rh−S−Rh hinge angles of 87.10(3) and 87.93(3)° and a Rh−Rh separation of 3.304 Å.[20] The η^1-thiapentadienyl ligands adopt a "syn exo" orientation, in which they are both directed *away from* the PEt_3 ligands for steric reasons (the torsional angle C4−S1−S2−C54 is 3.8°). The thiapentadienyl ligand planes are essentially perpendicular to one another (the dihedral angle between the planes C1/C2/C3/C4/S1 and C51/C52/C53/C54/S2 is 102.9°), and the ligands themselves are both W-shaped with trans geometries around the internal double bonds: C3−C4 and C53−C54. When **9** is treated with excess PEt_3 at room temperature in tetrahydrofuran, it readily converts back to **8**, which strongly implies that the η^1-thiapentadienyl ligand in **8** also possesses a trans internal double bond (vide supra). As shown in Scheme 6, when compound **8** is stirred in the noncoordinating solvent toluene at room temperature, a *different* sulfur-bridged dimer, [((1,4,5-η)-2,3-dimethyl-5-thiapentadienyl)$Rh(PEt_3)_2]_2$ (**10**), is gradually formed. Compound **10** is generated as a pair of noninterconverting isomers, "trans" **10a** and "cis" **10b**, in an approximate 4:1 ratio (see Chart 2). In these dimers, as in compound **3** (vide supra), the thiapentadienyl ligand has rearranged so that the carbon end of the chain (C1) is σ-bonded to rhodium, while the sulfur end (C4−S double bond) is π-bound. As before, an (η^5-thiapentadienyl)$Rh(PR_3)_2$ species (**F**; Scheme 6) appears to be a likely intermediate. The

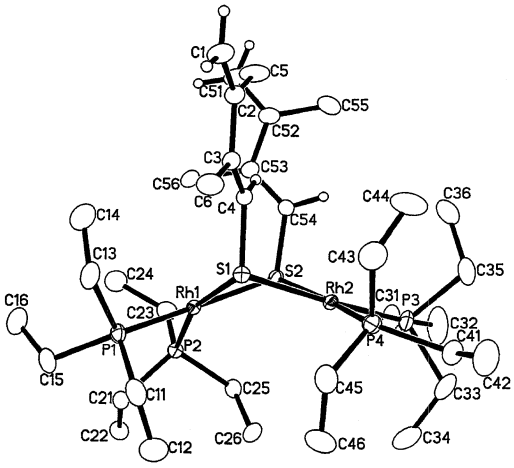

Figure 6. ORTEP drawing of **9**, using thermal ellipsoids at the 30% level. Methyl and ethyl H's are not shown. Selected bond distances (Å): Rh1−P1, 2.2470(9); Rh1−P2, 2.2533(9); Rh1−S1, 2.3850(8); Rh1−S2, 2.3722(8); C1−C2, 1.335(5); C2−C3, 1.465(4); C3−C4, 1.346(4); C4−S1, 1.765(3); Rh2−P3, 2.2378(9); Rh2−P4, 2.2466(9); Rh2−S1, 2.4111(8); Rh2−S2, 2.3876(8); C51−C52, 1.337(5); C52−C53, 1.476(5); C53−C54, 1.348(4); C54−S2, 1.753(3).

(20) The bending is due to the sulfur's preference to be highly pyramidalized and to the presence of a weak Rh−Rh bonding interaction: Oster, S. S.; Jones, W. D. *Inorg. Chim. Acta* **2004**, *357*, 1836.

Scheme 6

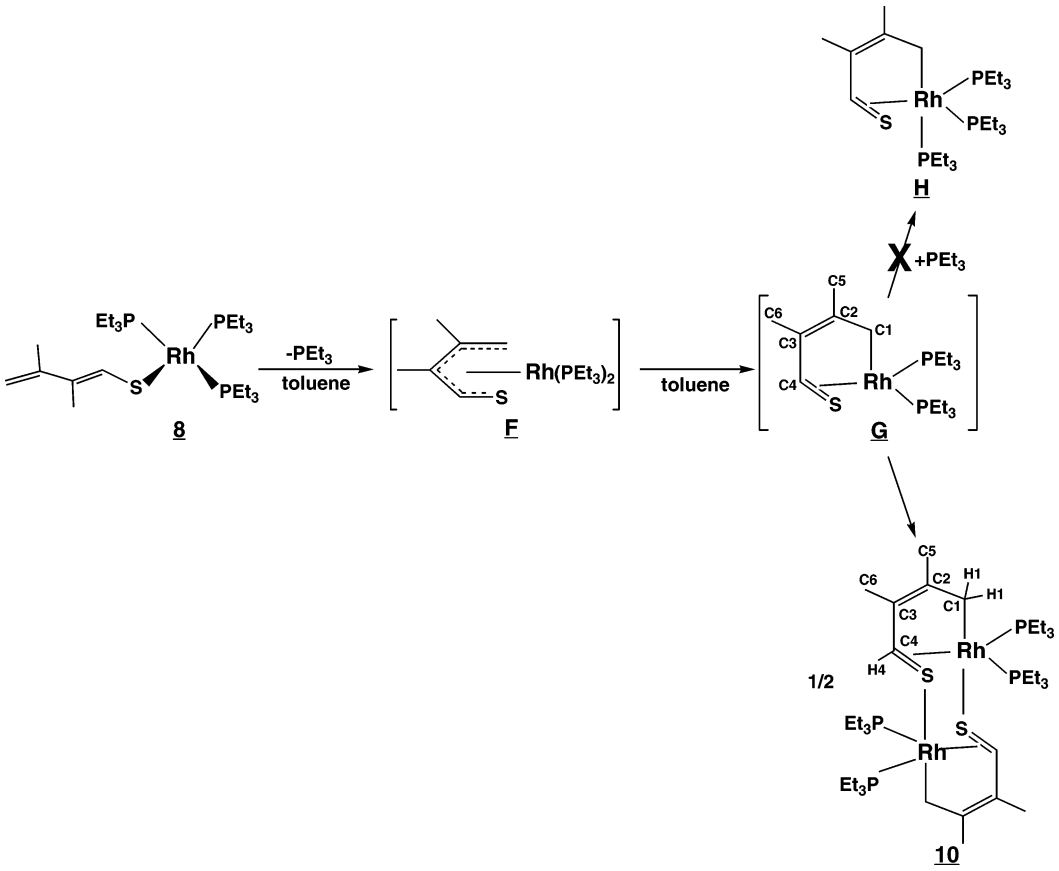

Chart 2

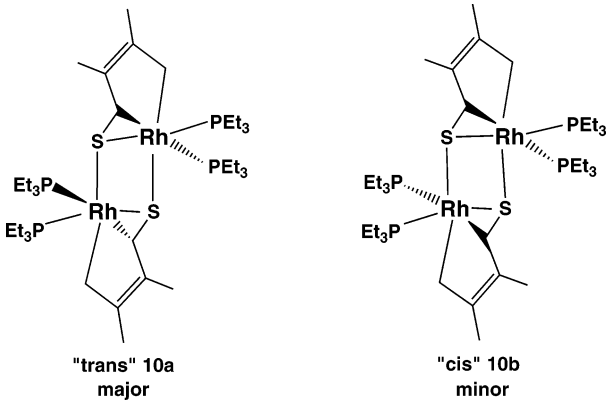

steric bulk of triethylphosphine promotes *dimerization* to **10** rather than ligand readdition to form the monomeric $(PEt_3)_3$ analogue of **3** (**H**; Scheme 6).

A close look at the monomeric building block of **10** (species **G**; Scheme 6) reveals that it is chiral (C4 is a chiral center). When different enantiomers of this monomeric unit combine, the trans dimer **10a** is produced, but when identical enantiomers combine, the cis dimer **10b** results. Hence the trans dimer is meso, while the cis dimer exists as a racemic mixture of *dd*/*ll* pairs.

The ^{1}H and ^{13}C{^{1}H} NMR spectra of dimers **10a**,**b** are very similar to those of compound **3**. In **10a**, for example, the signal for H4 appears at δ 4.55, while the two H1's resonate at δ 1.12 and 0.85. The π-bound carbon C4 appears at δ 76.4, while the σ-bound carbon C1 resonates at δ 23.7 and uncoordinated carbons C2 and C3 resonate at δ 138.9 and 137.8. The ^{31}P{^{1}H} NMR spectrum of the trans dimer **10a** consists of two doublet-of-doublets patterns, where the larger splitting is due to rhodium−phosphorus coupling and the smaller separation is due to phosphorus−phosphorus coupling. The more downfield ^{31}P signal, which is due to the phosphine trans to sulfur, exhibits a substantially larger J_{Rh-P} value than the upfield ^{31}P signal, which is due to the phosphine trans to C4 (166.7 Hz vs 119.8 Hz). The ^{31}P{^{1}H} NMR of cis dimer **10b** is similar to that of **10a**, but the line shapes are a bit more complicated, due to long-range coupling between phosphorus nuclei on the halves of the dimer.

The structure of trans dimer **10a** has been confirmed by X-ray diffraction and is presented in Figure 7.[21] The dimeric molecule sits on a crystallographically imposed inversion center, and the coordination geometry around each rhodium is best described as distorted octahedral. Ring carbon C1 and the bridging sulfur of the other monomer (S1′) occupy trans-diaxial sites, while C4, S1, P1, and P2 occupy equatorial sites. The carbon−carbon bonds within the thiapentadienyl ligand exhibit the expected single−double−single alternation, and the carbon−sulfur bond distance of 1.783(2) Å is close to that of a typical single bond (1.82 Å).[16] This C−S bond distance suggests strong π-back-bonding into the C−S π* orbital, and the Rh1−S1−C4 interaction can be viewed as a metallathiacyclopropane. Phosphorus atom P1, which is situated trans to sulfur S1, displays a significantly shorter bond to rhodium than does P2, which lies trans to C4 (2.2721(6) Å vs 2.3559(7) Å). This is consistent with the Rh−P coupling constants discussed above.

While we have not been able to obtain pure single crystals of cis isomer **10b**, the PMe_3 analogue of **10b**, *cis*-[((1,4,5-η)-2,3-dimethyl-5-thiapentadienyl)Rh(PMe_3)$_2$]$_2$ (**11b**), *has* been

(21) Earlier, we reported the structure of **10a**·(methylene chloride), which was crystallized from CH_2Cl_2 solvent.[1]

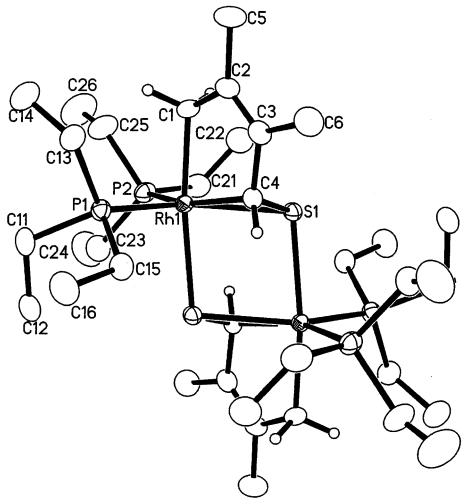

Figure 7. ORTEP drawing of **10a**, using thermal ellipsoids at the 50% level. Methyl and ethyl H's are not shown. Selected bond distances (Å): Rh1−P1, 2.2721(6); Rh1−P2, 2.3559(7); Rh1−S1, 2.4102(6); Rh1−S1′, 2.4729(6); Rh1−C1, 2.101(2); Rh1−C4, 2.077(2); C1−C2, 1.502(4); C2−C3, 1.335(4); C3−C4, 1.488(3); C4−S1, 1.783(2).

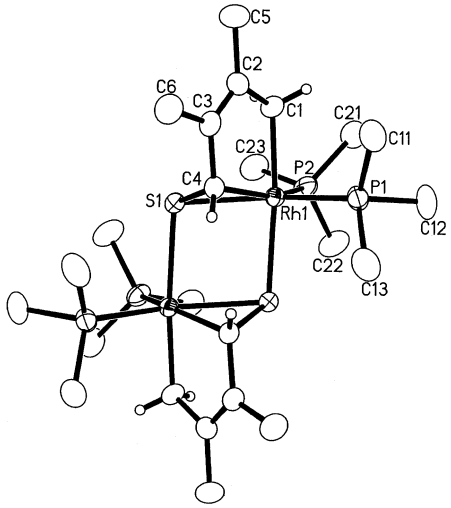

Figure 8. ORTEP drawing of **11b**, using thermal ellipsoids at the 50% level. Methyl H's are not shown. Selected bond distances (Å): Rh1−P1, 2.2593(9); Rh1−P2, 2.3141(9); Rh1−S1, 2.3906(8); Rh1−S1′, 2.4664(7); Rh1−C1, 2.107(3); Rh1−C4, 2.085(3); C1−C2, 1.495(6); C2−C3, 1.329(5); C3−C4, 1.492(5); C4−S1, 1.782(4).

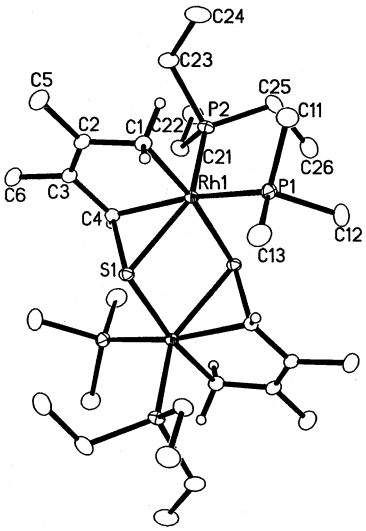

Figure 9. ORTEP drawing of **12a**, using thermal ellipsoids at the 30% level. Methyl and ethyl H's are not shown. Selected bond distances (Å): Rh1−P1, 2.3229(5); Rh1−P2, 2.2708(5); Rh1−S1, 2.4075(5); Rh1−S1′, 2.4534(5); Rh1−C1, 2.0987(18); Rh1−C4, 2.0758(18); C1−C2, 1.501(3); C2−C3, 1.333(3); C3−C4, 1.493(3); C4−S1, 1.7891(18).

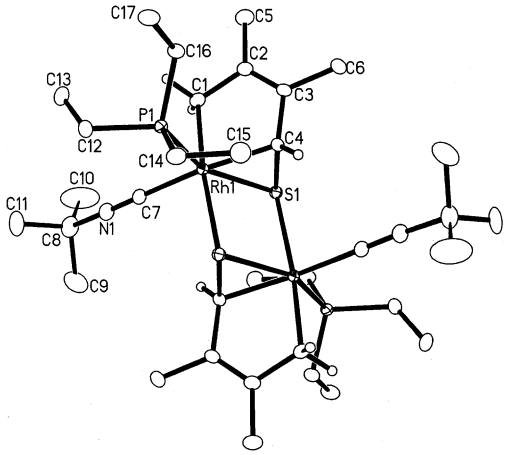

Figure 10. ORTEP drawing of **13a**, using thermal ellipsoids at the 50% level. Methyl and ethyl H's are not shown. Selected bond distances (Å): Rh1−P1, 2.2568(3); Rh1−C7, 1.9831(13); Rh1−S1, 2.3859(3); Rh1−S1′, 2.4531(3); Rh1−C1, 2.0990(12); Rh1−C4, 2.0758(12); C7−N1, 1.1547(16); N1−C8, 1.4523(18); C1−C2, 1.5071(18); C2−C3, 1.3388(19); C3−C4, 1.4901(17); C4−S1, 1.7968(12).

obtained (see the Experimental Section), and its X-ray crystal structure is presented in Figure 8. In this case, the dimer sits on a crystallographically imposed 2-fold rotation axis, which passes through the center of the Rh1−S1−Rh1′−S1′ rhomboid. The bond distance and angle data for **11b** are very similar to those of **10a**. It should be noted that, in compounds **10** and **11**, dimerization (i.e., sulfur bridge formation) occurs at the site opposite thiapentadienyl carbon C1. Not surprisingly, this is the same site that exhibits the longest Rh−P bond distance and the weakest rhodium−phosphorus NMR coupling (and, by implication, the weakest Rh−P interaction) in compound **3** (vide supra).

D. Reaction Chemistry of (Thiapentadienyl)(triethylphosphine)rhodium Complexes. As discussed above, the synthesis of [((1,4,5-η)-2,3-dimethyl-5-thiapentadienyl)Rh(PEt_3)$_2$]$_2$ (**10**) leads to a mixture of trans (**10a**) and cis (**10b**) isomers. Crystallization produces pure trans isomer (**10a**), which does *not* convert back to the isomeric mixture upon stirring in polar or nonpolar solvents. This result implies that the dimer cannot split up into (η^3-thiapentadienyl)Rh(PEt_3)$_2$ monomers in solution.

Compound **10a** does, however, react with small (sterically undemanding) ligands, L, to produce new mixed dimers of formula [((1,4,5-η)-2,3-dimethyl-5-thiapentadienyl)Rh(PEt_3)(L)]$_2$. For example, treatment of **10a** with excess PMe_3 in tetrahydrofuran produces [((1,4,5-η)-2,3-dimethyl-5-thiapentadienyl)Rh(PEt_3)(PMe_3)]$_2$, as the trans isomer **12a** (see Scheme 7). As expected, the NMR spectra of **12a** bear a very strong resemblance to those of **10a**. From a comparison of the ^{31}P{^{1}H} NMR spectra of **10a** and **12a**, it is possible to ascertain *which* of the two inequivalent PEt_3 ligands in **10a** has been replaced. The more downfield signal in **10a**'s ^{31}P{^{1}H} NMR spectrum (which is due to the phosphine trans to sulfur) is still there in **12a**'s ^{31}P{^{1}H} NMR spectrum, but the more upfield signal (which is due to the phosphine trans to C4) is gone and

Scheme 7

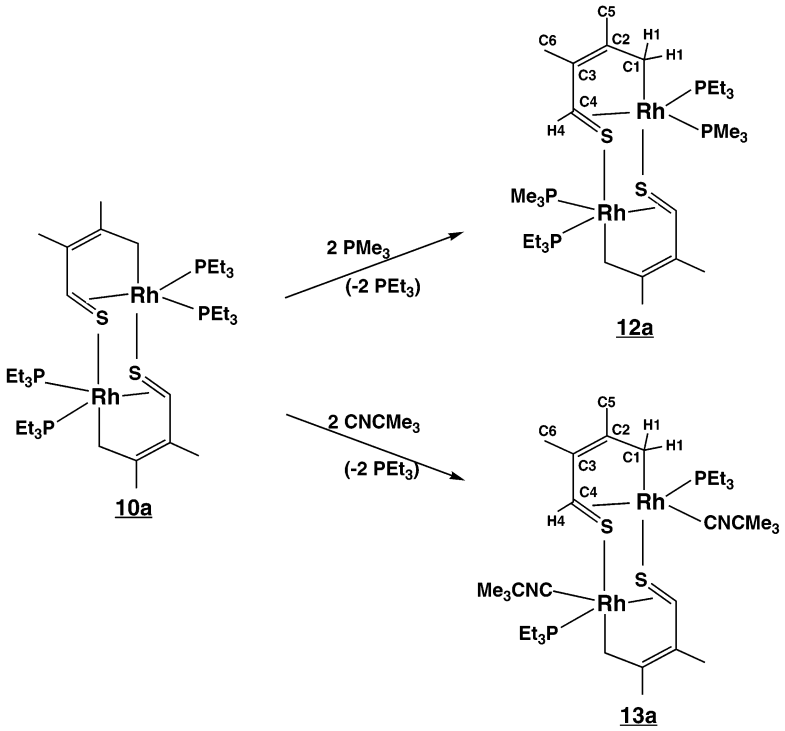

is replaced by a new signal in the PMe_3 region of the spectrum, indicating that the PEt_3 ligand trans to C4 has been replaced by PMe_3 in the mixed dimer. This is not surprising, given the fact that the phosphine trans to C4 has a significantly longer (weaker) bond to rhodium than the phosphine trans to S1 in the X-ray crystal structure of starting material **10a** and a substantially smaller Rh−P coupling constant in the $^{31}P\{^1H\}$ NMR spectrum (vide supra). Similarly, when **10a** is treated with excess *tert*-butyl isocyanide, the mixed dimer [((1,4,5-η)-2,3-dimethyl-5-thiapentadienyl)Rh(PEt_3)($CNCMe_3$)]$_2$ (**13a**), is produced cleanly (see Scheme 7). Again, the downfield signal remains in the $^{31}P\{^1H\}$ NMR spectrum of **13a**, while the upfield signal is gone, indicating that the PEt_3 ligand trans to C4 has been replaced by *tert*-butyl isocyanide.

The X-ray crystal structures of both **12a** and **13a** have been obtained and are presented in Figures 9 and 10, respectively. In each case, the molecule sits on a crystallographically imposed inversion center and retains the trans stereochemistry of the starting material. As predicted from the ^{31}P NMR data, the added ligands reside trans to thiapentadienyl carbon C4.

Given that the rhodium atoms in **10a** are 18e centers and that the dimeric structure cannot split up into monomers (vide supra), it appears that these ligand substitution reactions are *dissociative*. Dissociation of a bulky PEt_3 ligand produces a 16e metal center, which quickly adds a sterically less demanding ligand to generate the observed mixed-dimer products. With the removal of the steric driving force, additional PEt_3 ligand dissociations are disfavored, and no further ligand substitutions are observed, even upon heating in the presence of excess L.

Summary

This study demonstrates that the thiapentadienyl ligands in (thiapentadienyl)(phosphine)rhodium complexes can adopt a variety of bonding modes and that interconversions between these modes are facile. In general, thiapentadienyl bonding modes in which the *sulfur* atom is σ-bonded to the rhodium center (1,2,5-η^3 or 5-η^1) appear to be less thermodynamically stable than the 1,4,5-η^3 bonding mode, wherein the *carbon* end of the thiapentadienyl ligand is σ-bonded to rhodium. The thiapentadienyl ligands are reactive toward simple electrophiles, and the site of electrophilic addition changes with the electrophile. Specifically, H^+ is directed toward C1 of the thiapentadienyl chain (probably via the metal center) while Me^+ attacks the nucleophilic sulfur center. A recurring theme in this study is the formation of dimers through the agency of thiapentadienyl sulfur bridges. In some cases, these species form reversibly, while in others the strength of the Rh−S bridging bonds prevents dimer cleavage.

Research in the area of (heteropentadienyl)metal chemistry continues in our group, with the intent of learning more about the reactivity of these unique molecules. Particularly intriguing is the possibility of using heteropentadienyl ligand shifts to open and close coordination sites in a catalytic cycle, and work toward this end is ongoing.

Experimental Section

General Comments. All manipulations were carried out under a nitrogen atmosphere, using either glovebox or double-manifold Schlenk techniques. Solvents were stored under nitrogen after being distilled from the appropriate drying agents. Deuterated NMR solvents were obtained in sealed vials and used as received, except for CD_2Cl_2, which was passed through neutral alumina to remove acid impurities. The following reagents were used as obtained from the supplier indicated: $RhCl_3 \cdot 3H_2O$ (Pressure Chemical), cyclooctene (Aldrich), trimethylphosphine (Aldrich), triethylphosphine (Aldrich), tetrafluoroboric acid−diethyl etherate (Fluka), methyl trifluoromethane sulfonate (Aldrich), *tert*-butyl isocyanide (Aldrich).

(Cl)Rh(PMe_3)$_3$ and (Cl)Rh(PEt_3)$_3$ were obtained by adding 6 equiv of PMe_3 or PEt_3 to [(C_8H_{14})$_2$Rh(μ-Cl)]$_2$.[22] In each case, the phosphine addition was carried out at −30 °C, and the solution was stirred while slowly being warmed to room temperature. After

(22) Van der Ent, A.; Onderdelinden, A. L. *Inorg. Synth.* **1973**, *14*, 92.

filtration, the volatiles were removed under vacuum. Lithium 2,3-dimethyl-5-thiapentadienide was prepared by the literature procedure.[12]

NMR experiments were performed on a Varian Unity Plus-300 spectrometer (^{1}H, 300 MHz; ^{13}C, 75 MHz; ^{31}P, 121 MHz), a Varian Mercury-300 spectrometer (^{1}H, 300 MHz; ^{13}C, 75 MHz; ^{31}P, 121 MHz), a Varian Unity Plus-500 spectrometer (^{1}H, 500 MHz; ^{13}C, 125 MHz; ^{31}P, 202 MHz), or a Varian Unity-600 spectrometer (^{1}H, 600 MHz; ^{13}C, 150 MHz; ^{31}P, 242 MHz). ^{1}H and ^{13}C spectra were referenced to tetramethylsilane, while ^{31}P spectra were referenced to external H_3PO_4. HMQC (^{1}H-detected multiple quantum coherence) and HMBC (heteronuclear multiple-bond correlation) experiments aided in assigning some of the ^{1}H and ^{13}C peaks. Thiapentadienyl chain carbons are numbered C1−C4, with C1 on the side of the chain opposite sulfur. Methyl carbon C5 is bonded to C2, while methyl carbon C6 is bonded to C3.

Microanalyses were performed by Galbraith Laboratories, Inc., Knoxville, TN.

Synthesis of CH_2═C(Me)C(Me)═CHSRh(PMe_3)$_3$ (1). (Cl)-Rh(PMe_3)$_3$ (0.650 g, 1.77 mmol) was dissolved in 20 mL of tetrahydrofuran (THF) and cooled to −30 °C, forming a light orange solution. This solution was added to a −30 °C stirred solution of lithium 2,3-dimethyl-5-thiapentadienide (0.213 g, 1.77 mmol) in 15 mL of THF. The resulting solution was warmed to room temperature and stirred for an additional 30 min, during which time the color changed from light orange to dark reddish brown. The volatiles were removed in vacuo, resulting in a dry reddish brown film of **1**. This residue was redissolved in pentane and filtered before removal of the volatiles in vacuo. Crystals of compound **1** were obtained from concentrated solutions of toluene at −30 °C. Yield of **1**: 0.508 g (65%). Anal. Calcd for $C_{15}H_{36}P_3RhS$: C, 40.54; H, 8.18. Found: C, 40.46; H, 7.97. ^{1}H NMR (toluene-d_8, −20 °C): δ 5.74 (d, J_{H-P} = 9.6 Hz, 1, H4), 2.53 (s, 1, H1), 2.21 (d, J_{H-P} = 7.8 Hz, 1, H1), 2.18 (s, 3, H6's), 1.82 (br s, 3, H5's), 1.25 (br s, 18, PMe_3's), 0.87 (d, J_{H-P} = 7.8 Hz, 9, PMe_3). ^{13}C{^{1}H} NMR (toluene-d_8, −20 °C): δ 139.4 (s, C3), 121.8 (q, J_{C-P} = 4.3 Hz, C4), 73.3 (q, J_{C-P} = 12.0 Hz, C2), 43.9 (q, J_{C-P} = 11.0 Hz, C1), 28.8 (s, C5), 20.9 (br s, PMe_3's), 20.3 (partially obscured, C6). ^{31}P{^{1}H} NMR (toluene-d_8, 22 °C): δ −1.0 (dt, J_{P-Rh} = 126.0 Hz, J_{P-P} = 36.1 Hz, 1, PMe_3), −22.7 (dd, J_{P-Rh} = 122.1 Hz, J_{P-P} = 36.1 Hz, 2, PMe_3's).

Synthesis of CH_2═C(Me)C(Me)═CHSRh(PMe_3)$_3$(η^2-O_2) (2). Compound **1**, CH_2═C(Me)C(Me)═CHSRh(PMe_3)$_3$ (0.116 g, 0.261 mmol), was dissolved in 50 mL of acetone at −30 °C, forming a light yellow solution. The solution was then stirred in air at 0 °C for 20 min, during which time the color of the solution turned to reddish brown. The volatiles were removed in vacuo, resulting in a dry reddish brown film of **2**. Needle-shaped crystals of compound **2** were obtained from concentrated solutions of acetone at −30 °C. Yield of **2**: 0.099 g (80%). Anal. Calcd for $C_{15}H_{36}O_2P_3RhS$: C, 37.80; H, 7.62. Found: C, 37.42; H, 7.60. ^{1}H NMR (acetone-d_6, 22 °C): δ 6.51 (s, 1, H4), 5.12 (d, J = 2.1 Hz, 1, H1), 4.83 (s, 1, H1), 2.13 (m, 3, H5's), 1.79 (d, J = 1.2 Hz, 3, H6's), 1.54 (d, J_{H-P} = 9.3 Hz, 9, eq PMe_3), 1.43 (virtual t, J_{H-P} = 6.9 Hz, 18, ax PMe_3's). ^{13}C{^{1}H} NMR (acetone-d_6, 22 °C): δ 146.2 (s, C2 or C3), 138.9 (s, C4), 129.8 (s, C2 or C3), 111.7 (s, C1), 25.1 (s, C6), 24.4 (s, C5), 20.1 (d, J_{C-P} = 28.2 Hz, eq PMe_3), 12.6 (virtual t, J_{C-P} = 30.8 Hz, ax PMe_3's). ^{31}P{^{1}H} NMR (acetone-d_6, 22 °C): δ 0.1 (dd, J_{P-Rh} = 97.6 Hz, J_{P-P} ≈ 31 Hz, 2, ax PMe_3's), −2.4 (ddd, J_{P-Rh} = 138.5 Hz, J_{P-P} = 33.3 Hz, 29.9 Hz, 1, eq PMe_3). Note: the ddd pattern for the equatorial phosphine suggests that the two axial phosphines are chemically inequivalent, but the chemical shifts of the axial phosphines are essentially identical.

Synthesis of S═CHC(Me)═C(Me)CH_2Rh(PMe_3)$_3$ (3). Compound **1**, CH_2═C(Me)C(Me)═CHSRh(PMe_3)$_3$ (0.472 g, 1.06 mmol), was dissolved in tetrahydrofuran. The resulting orange solution was stirred at room temperature for 2 days, during which time the color changed from orange to brown. After the volatiles were removed in vacuo, the resulting brown residue was dissolved in a minimal quantity of acetone and cooled to −30 °C, causing **3** to crystallize as yellow needles. Yield of **3**: 0.472 g (100%). Anal. Calcd for $C_{15}H_{36}P_3RhS$: C, 40.54; H, 8.18. Found: C, 40.46; H, 7.97. ^{1}H NMR (toluene-d_8, −20 °C): δ 4.09 (br s, 1, H4), 2.25 (br s, 1, H1), 2.05 (s, 3, H6's), 1.80 (s, 3, H5's), 1.10 (v br s, 1, H1), 1.05 (d, J_{H-P} = 6.0 Hz, 9, PMe_3), 0.96 (d, J_{H-P} = 9.0 Hz, 9, PMe_3), 0.94 (d, J_{H-P} = 7.2 Hz, 9, PMe_3). ^{13}C{^{1}H} NMR (toluene-d_8, −20 °C): δ 142.0 (s, C2 or C3), 136.0 (d of m, J_{C-P} = 14.6 Hz, C2 or C3), 73.6 (dd, J_{C-P} = 45.9 Hz, 14.6 Hz, C4), 32.2 (d of m, J_{C-P} = 98.8 Hz, C1), 20.9 (partially obscured, C5), 20.0 (s, C6), 20.0 (d, J_{C-P} = 16.5 Hz, PMe_3), 19.5 (d, J_{C-P} = 22.0 Hz, PMe_3), 16.5 (d, J_{C-P} = 20.1 Hz, PMe_3). ^{31}P{^{1}H} NMR (toluene-d_8, 22 °C): δ 0.0 (ddd, J_{P-Rh} = 162.9 Hz, J_{P-P} = 24.1 Hz, 24.1 Hz, 1, PMe_3 trans to S), −18.8 (ddd, J_{P-Rh} = 123.4 Hz, J_{P-P} = 28.0 Hz, 24.1 Hz, 1, PMe_3 trans to C4), −25.1 (ddd, J_{P-Rh} = 80.0 Hz, J_{P-P} = 28.0 Hz, 24.1 Hz, 1, PMe_3 trans to C1).

Synthesis of {[(η^4-Me_2C═C(Me)CH═S)Rh(PMe_3)$_2$]$_2$}$^{2+}$(BF_4^-)$_2$ (4). Compound **1**, CH_2═C(Me)C(Me)═CHSRh(PMe_3)$_3$ (0.199 g, 0.449 mmol), was dissolved in 100 mL of diethyl ether at −75 °C to form a yellow solution. HBF_4·OEt_2, 51−57% assay (0.145 g, 0.449 mmol), was added via syringe, causing the solution color to change to dark brown. The solution was stirred at ambient temperature for 15 min, during which time a fine dull yellow powder of compound **4** precipitated out of the solution. The dull yellow powder was isolated via filtration and crystallized as orange prisms from concentrated solutions of methylene chloride or acetone. Alternatively, a precipitate of compound **4** was formed by adding HBF_4·OEt_2 to a solution of compound **3** at −30 °C in tetrahydrofuran and stirring for 45 min. Yield of **4**: 0.096 g (47%). Anal. Calcd for $C_{24}H_{56}B_2F_8P_4Rh_2S_2$: C, 31.60; H, 6.20. Found: C, 31.25; H, 6.58. ^{1}H NMR (methylene chloride-d_2, 22 °C): δ 7.05 (d, J_{H-P} = 5.7 Hz, 1, H4), 2.44 (s, 3, H6's), 1.88 (d, J_{H-P} = 9.0 Hz, 9, PMe_3), 1.61 (d, J_{H-P} = 10.5 Hz, 9, PMe_3), 1.20 (d, J_{H-P} = 4.2 Hz, 3, H1's), 1.13 (d, J_{H-P} = 3.9 Hz, 3, H5's). ^{13}C{^{1}H} NMR (methylene chloride-d_2, 22 °C): δ 125.3 (s, C3), 104.3 (s, C4), 62.9 (s, C2), 29.0 (s, C1), 22.3 (s, C5), 20.0 (s, C6), 19.7 (d, J_{C-P} = 28.2 Hz, PMe_3), 17.6 (d, J_{C-P} = 32.1 Hz, PMe_3). ^{31}P{^{1}H} NMR (methylene chloride-d_2, 22 °C): δ 6.2 (complex dd, J_{P-Rh} = 119.6 Hz, J_{P-P} = 39.0 Hz, 1, PMe_3), −8.6 (dd, J_{P-Rh} = 156.4 Hz, J_{P-P} = 39.0 Hz, 1, PMe_3).

Synthesis of [(η^4-CH_2═C(Me)C(Me)═CHS(Me))Rh(PMe_3)$_3$]$^+$-$O_3SCF_3^-$ (5). Compound **1**, CH_2═C(Me)C(Me)═CHSRh(PMe_3)$_3$ (0.300 g, 0.675 mmol), was dissolved in 50 mL of diethyl ether at −75 °C to form a yellow solution. $CH_3O_3SCF_3$ (0.110 g, 0.675 mmol) was then added via syringe, resulting in a cloudy yellow solution. The solution was stirred for 15 min, during which time compound **5** precipitated out as a light yellow powder. The solution was warmed to room temperature, and the light yellow powder was isolated via filtration. Yield of **5**: 0.300 g (73%). Anal. Calcd for $C_{17}H_{39}F_3O_3P_3RhS_2$: C, 33.56; H, 6.46. Found: C, 33.82; H, 6.15. ^{1}H NMR (acetone-d_6, 22 °C): δ 3.42 (m, 1, H4), 2.67 (m, 1, H1), 2.37 (m, 1, H1), 2.18 (t, J = 2.4 Hz, 3, H5's), 2.16 (t, J = 4.2 Hz, 3, H6's), 2.11 (s, 3, S-Me), 1.69 (d, J_{H-P} = 9.6 Hz, 9, PMe_3), 1.52 (d, J_{H-P} = 8.4 Hz, 9, PMe_3), 1.46 (d, J_{H-P} = 7.8 Hz, 9, PMe_3). ^{13}C{^{1}H} NMR (acetone-d_6, 22 °C): δ 116.0 (s, C2), 101.8 (s, C3), 55.1 (d, J_{C-P} = 57.6 Hz, C4), 47.1 (d, J_{C-P} = 34.7 Hz, C1), 21.7 (d, J = 6.5 Hz, C5), 21.5 (dd, J = 26.8 Hz, 12.8 Hz, PMe_3), 21.2 (d, J = 7.7 Hz, C6 or *S*-Me), 21.0 (s, C6 or *S*-Me), 19.6 (dd, J = 24.3 Hz, 6.3 Hz, PMe_3), 19.2 (dd, J = 25.6 Hz, 8.9 Hz, PMe_3). ^{31}P{^{1}H} NMR (acetone-d_6, 22 °C): δ −7.7 (ddd, J_{P-Rh} = 158.0 Hz, J_{P-P} = 15.2 Hz, 11.1 Hz, 1, PMe_3), −14.3 (ddd, J_{P-Rh} = 117.5

Hz, J_{P-P} = 29.7 Hz, 11.1 Hz, 1, PMe_3), −17.3 (ddd, J_{P-Rh} = 106.0 Hz, J_{P-P} = 29.7 Hz, 15.2 Hz, 1, PMe_3).

Synthesis of $[(Me)S{=}CHC(Me){=}C(Me)CH_2Rh(PMe_3)_3]^+$-$O_3SCF_3^-$ (6). Compound **3**, $S{=}CHC(Me){=}C(Me)CH_2Rh(PMe_3)_3$ (0.21 g, 0.473 mmol), was dissolved in 20 mL of acetone at −30 °C, forming a light yellow solution. $CH_3O_3SCF_3$ (0.077 g, 0.473 mmol) was then added via syringe, causing the solution color to change to dark yellow. After the mixture was warmed to room temperature and stirred for 15 min, the volatiles were removed in vacuo. The light yellow solid was washed with cold pentane, redissolved in a minimal quantity of acetone, and cooled to −30 °C, causing compound **6** to crystallize as light yellow prisms. Yield of **6**: 0.230 g (80%). Anal. Calcd for $C_{17}H_{39}F_3O_3P_3RhS_2$: C, 33.56; H, 6.46. Found: C, 33.82; H, 6.15. ^{1}H NMR (acetone-d_6, 22 °C): δ 3.83 (t, J_{H-P} = 6.6 Hz, 1, H4), 1.82 (br s, 6, H5's and H6's), 1.75 (m, partially obscured, 1, H1), 1.63 (d, J_{H-P} = 5.4 Hz, 3, *S*-Me), 1.56 (dd, J_{H-P} = 7.8 Hz, 0.6 Hz, 9, PMe_3), 1.55 (m, partially obscured, 1, H1), 1.50 (dd, J_{H-P} = 9.6 Hz, 1.2 Hz, 9, PMe_3), 1.46 (d, J_{H-P} = 7.2 Hz, 9, PMe_3). ^{13}C{^{1}H} NMR (acetone-d_6, 22 °C): δ 149.4 (s, C2 or C3), 134.5 (s, C2 or C3), 64.7 (dd, J_{C-P} = 57.5 Hz, 15.3 Hz, C4), 36.7 (dd, J_{C-P} = 76.5 Hz, 19.0 Hz, C1), 19.7−19.4 (s's, partially obscured, C5 and C6), 19.4 (d, J_{C-P} = 23.0 Hz, PMe_3), 19.2 (d, J_{C-P} = 28.0 Hz, PMe_3), 17.0 (d, J_{C-P} = 23.0 Hz, PMe_3), 10.1 (d, J_{C-P} = 7.6 Hz, *S*-Me). ^{31}P{^{1}H} NMR (acetone-d_6, 22 °C): δ 8.9 (dd, J_{P-Rh} = 161.7 Hz, J_{P-P} = 28.2 Hz, 1, PMe_3 trans to S), −17.4 (dd, J_{P-Rh} = 112.9 Hz, J_{P-P} = 29.7 Hz, 1, PMe_3 trans to C4), −24.2 (ddd, J_{P-Rh} = 77.8 Hz, J_{P-P} = 29.7 Hz, 28.2 Hz, 1, PMe_3 trans to C1).

$\{(H_2C)[S{=}CHC(Me){=}C(Me)CH_2Rh(PMe_3)_3]_2\}^{2+}(Cl^-)_2$ (7). Compound **3**, $S{=}CHC(Me){=}C(Me)CH_2Rh(PMe_3)_3$ (0.0800 g, 0.180 mmol), was dissolved in 25 mL of methylene chloride at −30 °C. The resulting light yellow solution was stirred at room temperature for 15 min, during which time the color changed to light red. The volatiles were removed in vacuo, resulting in an off-white powder of compound **7**. This off-white powder was washed with cold pentane, redissolved in methylene chloride, and cooled to −30 °C, causing compound **7** to crystallize as off-white prisms. Yield of **7**: 0.057 g (65%). Anal. Calcd for $C_{31}H_{74}Cl_2P_6Rh_2S_2$: C, 38.24; H, 7.66. Found: C, 37.94; H, 7.42. ^{1}H NMR (methylene chloride-d_2, −20 °C): δ 3.84 (br t, 1, H4), 2.22 (s, 2, CH_2), 1.87 (s, 3, H6's), 1.75 (s, 3, H5's), ∼1.6 (m, partially obscured, 1, H1), ∼1.4 (m, obscured, 1, H1), 1.41 (d, J_{H-P} = 7.2 Hz, 9, PMe_3), 1.37 (d, J_{H-P} = 10.2 Hz, 9, PMe_3), 1.35 (d, J_{H-P} = 7.2 Hz, 9, PMe_3). ^{13}C{^{1}H} NMR (methylene chloride-d_2, −20 °C): δ 150.7 (s, C2 or C3), 133.7 (s, C2 or C3), 64.5 (d, J_{C-P} = 58.6 Hz, C4), 34.3 (d, J_{C-P} = 74.0 Hz, C1), 24.4 (br s, CH_2), 20.1 (s, C6), 19.7 (s, C5), 19.4 (d, J_{C-P} = 24.2 Hz, PMe_3), 19.0 (d, J_{C-P} = 31.9 Hz, PMe_3), 16.6 (d, J_{C-P} = 23.0 Hz, PMe_3). ^{31}P{^{1}H} NMR (methylene chloride-d_2, 22 °C): δ 12.7 (dd, J_{P-Rh} = 161.4 Hz, J_{P-P} = 27.3 Hz, 1, PMe_3 trans to S), −14.4 (dd, J_{P-Rh} = 112.1 Hz, J_{P-P} = 29.3 Hz, 1, PMe_3 trans to C4), −23.0 (ddd, J_{P-Rh} = 76.8 Hz, J_{P-P} = 29.3 Hz, 27.3 Hz, 1, PMe_3 trans to C1).

Synthesis of $CH_2{=}C(Me)C(Me){=}CHSRh(PEt_3)_3$ (8). (Cl)Rh-$(PEt_3)_3$ (0.644 g, 1.31 mmol) was dissolved in 15 mL of tetrahydrofuran (THF) at −30 °C, forming a deep orange solution. This solution was added to a −30 °C stirred solution of lithium 2,3-dimethyl-5-thiapentadienide (0.157 g, 1.31 mmol) in 15 mL of THF. The reaction mixture was warmed to room temperature and stirred for 1 h, during which time the color changed from deep orange to reddish brown. The volatiles were removed in vacuo, and the resulting oily brown residue was extracted with pentane and filtered to give a solution of compound **8**. Compound **8** was stabilized in solution by adding triethylphosphine, which retarded the subsequent formation of compound **10**. Alternatively, compound **8** was formed by adding excess PEt_3 to a solution of compound **9** in THF and stirred for 24 h. Yield of **8**: 0.642 g (86%). Note: the instability of compound **8** toward formation of dimer **10** prevented acquisition of an accurate elemental analysis. ^{1}H NMR (toluene-d_8, 22 °C): δ 7.22 (d, J_{H-P} = 3.6 Hz, 1, H4), 4.95 (d, J = 2.1 Hz, 1, H1), 4.80 (br s, 1, H1), 2.40 (s, 3, H6's), 2.13 (s, 3, H5's), 1.79−1.69 (m, 12, PEt_3 CH_2's), 1.39 (dq, J_{H-P} = 7.2 Hz, J_{H-H} = 7.2 Hz, 6, PEt_3 CH_2's), 1.07−0.91 (m, 27, PEt_3 CH_3's). ^{13}C{^{1}H} NMR (toluene-d_8, 22 °C): δ 144.5 (s, C2 or C3), 137.7 (s, C4), 130.1 (s, C2 or C3), 105.0 (s, C1), 21.5 (s, C5), 21.2 (d, J_{C-P} = 21.9 Hz, PEt_3 CH_2's), 17.9 (virtual t, J_{C-P} = 23.6 Hz, PEt_3 CH_2's), 15.0 (s, C6), 9.5 (s, PEt_3 CH_3's), 9.2 (s, PEt_3 CH_3's). ^{31}P{^{1}H} NMR (toluene-d_8, 22 °C): δ 31.3 (dt, J_{P-Rh} = 161.8 Hz, J_{P-P} = 38.1 Hz, 1, PEt_3), 18.0 (dd, J_{P-Rh} = 138.9 Hz, J_{P-P} = 38.1 Hz, 2, PEt_3's).

Synthesis of $[CH_2{=}C(Me)C(Me){=}CHSRh(PEt_3)_2]_2$ (9). (Cl)-$Rh(PEt_3)_3$ (0.837 g, 1.70 mmol) was dissolved in 15 mL of tetrahydrofuran (THF) to form a deep orange solution and then cooled to −30 °C. This solution was added to a −30 °C stirred solution of lithium 2,3-dimethyl-5-thiapentadienide (0.204 g, 1.70 mmol) in 15 mL of THF. The resulting solution was warmed to room temperature and stirred for an additional 1 h, during which time the color changed from deep orange to reddish brown. The volatiles were removed in vacuo, and the resulting oily brown residue was extracted with pentane and filtered. The solvent was again removed in vacuo, and the residue was redissolved in acetone, causing a small quantity of compound **10** to precipitate out as a yellow powder. The yellow powder was removed from the solution via filtration, and the resulting supernatant was allowed to sit at room temperature for 24 h, during which time compound **9** precipitated out as an orange powder. This orange powder was washed with cold diethyl ether, redissolved in a minimal quantity of pentane, and cooled to −30 °C, causing compound **9** to crystallize as orange prisms. Yield of **9**: 0.645 g (84%). Anal. Calcd for $C_{36}H_{78}P_4Rh_2S_2$: C, 47.78; H, 8.71. Found: C, 47.82; H, 8.35. ^{1}H NMR (tetrahydrofuran-d_8, 22 °C): δ 6.96 (s, 1, H4), 4.74 (s, 1, H1), 4.66 (s, 1, H1), 2.39 (s, 3, H6's), 1.84 (s, 3, H5's), 1.62 (br s, 12, PEt_3 CH_2's), 1.13 (br s, 18, PEt_3 CH_3's). ^{13}C{^{1}H} NMR (tetrahydrofuran-d_8, 22 °C): δ 146.2 (s, C2 or C3), 134.7 (s, C2 or C3), 133.7 (s, C4), 107.8 (s, C1), 21.7 (s, C5), 19.4 (virtual t, J_{C-P} = 23.2 Hz, PEt_3 CH_2's), 17.3 (s, C6), 9.5 (s, PEt_3 CH_3's). ^{31}P{^{1}H} NMR (tetrahydrofuran-d_8, 22°C): δ31.8 (d, J_{P-Rh} = 168.5 Hz, PEt_3's).

Synthesis of $[S{=}CHC(Me){=}C(Me)CH_2Rh(PEt_3)_2]_2$ (10). (Cl)-$Rh(PEt_3)_3$ (1.20 g, 2.44 mmol) was dissolved in 15 mL of tetrahydrofuran (THF) to form a deep orange solution and then cooled to −30 °C. This solution was added to a −30 °C stirred solution of lithium 2,3-dimethyl-5-thiapentadienide (0.295 g, 2.44 mmol) in 15 mL of THF. The reaction mixture was warmed to room temperature and stirred for 1 h, during which time the color changed from deep orange to reddish brown. The volatiles were removed in vacuo, and the resulting oily brown residue was extracted with pentane and the extract filtered. After removal of the pentane in vacuo, the residue was redissolved in toluene. Compound **10** slowly precipitated out of this solution at room temperature as a yellow powder. The yellow powder was isolated via filtration and crystallized as shiny yellow plates from concentrated solutions of methylene chloride at −30 °C. Yield of **10**: 0.933 g (84%). Anal. Calcd for $C_{36}H_{78}P_4Rh_2S_2$: C, 47.78; H, 8.71. Found: C, 47.82; H. 8.35.

NMR of trans isomer **10a**: ^{1}H NMR (methylene chloride-d_2, 22 °C) δ 4.55 (t, J_{H-P} = 4.5 Hz, 1, H4), 2.02 (complex m, 6, PEt_3 CH_2's), 1.77 (s, 3, H6's), 1.70 (complex m, 6, PEt_3 CH_2's), 1.32 (s, 3, H5's), 1.20 (dt, J_{H-P} = 15.0 Hz, J_{H-P} = 7.5 Hz, 9, PEt_3 CH_3's), 1.12 (br m, 1, H1), 1.06 (dt, J_{H-P} = 15.0 Hz, J_{H-H} = 7.5 Hz, 9, PEt_3 CH_3's), 0.85 (br m, 1, H1); ^{13}C{^{1}H} NMR (methylene chloride-d_2, −20 °C) δ 138.9 (d, J_{C-P} = 5.1 Hz, C2 or C3), 137.8 (d, J_{C-P} = 11.6 Hz, C2 or C3), 76.4 (d, J_{C-P} = 55.1 Hz, C4), 23.7 (complex d, J_{C-P} = 21.9 Hz, C1), 19.7 (s, C5), 19.2 (d, J_{C-P} = 3.9

Table 1. X-ray Diffraction Structure Summary

	1	**2**	**3**	**4**	**7**
empirical formula	$C_{18.5}H_{40}P_3RhS$[a]	$C_{15}H_{36}O_2P_3RhS$	$C_{15}H_{36}P_3RhS$[b]	$C_{28}H_{64}B_2Cl_8F_8P_4Rh_2S_2$[c]	$C_{35}H_{86}Cl_{10}O_2P_6Rh_2S_2$[d]
fw	490.39	476.32	444.32	1251.83	1349.30
cryst syst	monoclinic	triclinic	monoclinic	triclinic	triclinic
space group	$I2/a$	$P\bar{1}$	$P2_1$	$P\bar{1}$	$P\bar{1}$
a, Å	19.1092(7)	7.8973(2)	8.3157(2)	11.1689(4)	10.6711(4)
b, Å	10.6599(4)	12.0464(3)	18.0517(3)	11.3509(4)	10.9528(5)
c, Å	23.8199(13)	13.4050(4)	14.4126(3)	11.9124(5)	14.1397(6)
α, deg	90	100.500(2)	90	62.969(2)	96.907(2)
β, deg	95.774(2)	104.930(1)	90.653(1)	69.949(2)	98.122(2)
γ, deg	90	108.531(1)	90	74.930(2)	109.458(2)
V, Å^3	4827.5(4)	1118.73(5)	2163.37(8)	1253.87(8)	1517.62(11)
Z	8	2	4	1	1
cryst dimens, mm	0.21 × 0.14 × 0.12	0.28 × 0.15 × 0.13	0.22 × 0.16 × 0.12	0.17 × 0.09 × 0.07	0.25 × 0.19 × 0.09
calcd density, g/cm^3	1.349	1.414	1.364	1.658	1.476
radiation; λ, Å	0.710 73	0.710 73	0.710 73	0.710 73	0.710 73
temp, K	165(2)	100(2)	165(2)	100(2)	170(2)
θ range, deg	2.09−28.00	1.64−33.19	1.81−26.99	1.96−25.36	2.00−26.00
data collected					
h	−25 to +25	−12 to +12	−10 to +10	−13 to +13	−13 to +13
k	−13 to +14	−18 to +18	−23 to +23	−13 to +13	−13 to +13
l	−31 to +31	−20 to +20	−18 to +18	−14 to +14	−17 to +16
total decay	none obsd	none obsd	none obsd	none obsd	none obsd
no. of data collected	72 023	44 034	43 228	19 280	12 903
no. of unique data	5816	8536	9386	4567	5945
Mo Kα linear abs coeff, mm^{-1}	0.993	1.075	1.100	1.347	1.239
abs cor applied	empirical (SADABS)	numerical	empirical (SADABS)	numerical	empirical (SADABS)
data to param ratio	27.96	42.89	25.30	15.80	17.54
final R indices (obsd data)[e]					
R1	0.0367	0.0245	0.0338	0.0618	0.0499
wR2	0.0851	0.0543	0.0645	0.1375	0.1074
R indices (all data)					
R1	0.0472	0.0333	0.0380	0.0887	0.0702
wR2	0.0897	0.0562	0.0655	0.1549	0.1152
goodness of fit	1.052	1.020	1.050	1.055	1.045

[a] Includes $^1/_2$ molecule of toluene. [b] Two independent molecules in the unit cell. [c] Includes 4 molecules of methylene chloride. [d] Includes 4 molecules of methylene chloride and 2 molecules of water.

Hz, C6), 18.9 (d, J_{C-P} = 20.5 Hz, PEt_3 CH_2's), 18.2 (d, J_{C-P} = 12.8 Hz, PEt_3 CH_2's), 8.9 (s, PEt_3 CH_3's), 8.4 (d, J_{C-P} = 3.8 Hz, PEt_3 CH_3's); $^{31}P\{^1H\}$ NMR (methylene chloride-d_2, 22 °C) δ 23.3 (ddd, J_{P-Rh} = 166.7 Hz, J_{P-P} = 14.8 Hz, J_{P-P} = 3.0 Hz, 1, PEt_3 trans to S), 7.7 (ddd, J_{P-Rh} = 119.8 Hz, J_{P-P} = 14.8 Hz, J_{P-P} = 3.0 Hz, 1, PEt_3 trans to C4).

Selected NMR peaks for cis isomer **10b**: ^1H NMR (methylene chloride-d_2, 22 °C) δ 4.94 (br t, 1, H4); $^{31}P\{^1H\}$ NMR (methylene chloride-d_2, 22 °C) δ 22.4 (d of complex m, $J_{P-Rh} \approx$ 170 Hz, 1, PEt_3 trans to S), 6.4 (d of "filled-in" d, J_{P-Rh} = 120.3 Hz, 1, PEt_3 trans to C4).

Synthesis of [S═CHC(Me)═C(Me)CH_2Rh$(PMe_3)_2]_2$ (11). (Cl)-$Rh(PMe_3)_3$ (1.10 g, 3.00 mmol) was dissolved in 100 mL of tetrahydrofuran (THF) to form a light orange solution and then cooled to −30 °C. This solution was added to a −30 °C stirred solution of lithium 2,3-dimethyl-5-thiapentadienienide (0.361 g, 3.00 mmol) in 15 mL of THF. The resulting dark reddish brown solution was stirred at room temperature for 3 days, during which time the color changed to brown. The volatiles were removed in vacuo, and the resulting orange-brown residue was redissolved in pentane, followed by filtration. The filtrate volatiles were removed in vacuo, and the residue was redissolved in acetone, resulting in formation of a fine yellow precipitate of compound **11**. The yellow powder was isolated via filtration and crystallized as shiny yellow plates from concentrated solutions of methylene chloride at −30 °C. Yield of **11**: 0.55 g (50%). Anal. Calcd for $C_{24}H_{54}P_4Rh_2S_2$: C, 39.14; H, 7.39. Found: C, 39.23; H, 7.13.

NMR of cis isomer **11b**: ^1H NMR (methylene chloride-d_2, 22 °C) δ 4.50 (br t, 1, H4), 1.72 (s, 3, H6's), 1.50 (d, J_{H-P} = 6.0 Hz, 9, PMe_3), 1.33 (s, 3, H5's), 1.32 (d, J_{H-P} = 8.0 Hz, 9, PMe_3), 0.97 (m, 1, H1), 0.69 (m, 1, H1); $^{13}C\{^1H\}$ NMR (methylene chloride-d_2, 22 °C) δ 137.5 (C2 and C3, s), 71.5 (br d, J_{C-P} = 55.4 Hz, C4), 25.3 (br d, J_{C-P} = 21.9 Hz, C1), 20.1 (s, C5), 19.4 (s, C6), 18.9 (d, J_{C-P} = 16.8 Hz, PMe_3), 16.6 (d, J_{C-P} = 23.5 Hz, PMe_3); $^{31}P\{^1H\}$ NMR (methylene chloride-d_2, 22 °C) δ 5.2 (d of complex m, $J_{P-Rh} \approx$ 165 Hz, 1, PMe_3 trans to S), −15.9 (d of "filled-in" d), J_{P-Rh} = 124.6 Hz, 1, PMe_3 trans to C4).

Selected NMR peaks for trans isomer **11a**: ^1H NMR (methylene chloride-d_2, 22 °C): δ 4.37 (t, J_{H-P} = 5.4 Hz, 1, H4); $^{31}P\{^1H\}$ NMR (methylene chloride-d_2, 22 °C) δ 3.5 (dd, J_{P-Rh} = 171.8 Hz, J_{P-P} = 12.2 Hz, 1, PMe_3 trans to S), −18.4 (dd, J_{P-Rh} = 120.9 Hz, J_{P-P} = 12.2 Hz, 1, PMe_3 trans to C4).

Synthesis of [S═CHC(Me)═C(Me)CH_2Rh$(PEt_3)(PMe_3)]_2$ (12a). Compound **10a**, [S═CHC(Me)═C(Me)CH_2Rh$(PEt_3)_2]_2$ (0.531 g, 0.587 mmol), was dissolved in 15 mL of tetrahydrofuran (THF) to form a deep yellow solution and then cooled to −30 °C. Excess PMe_3 (0.201 g, 2.64 mmol) was likewise cooled to −30 °C and added to the yellow solution of **10a**, causing the color to change to light yellow. After it was warmed to room temperature and stirred for 1 h, the solution was filtered and the volatiles were removed in vacuo. The yellowish brown residue was dissolved in a minimal quantity of methylene chloride and cooled to −30 °C, causing **12a** to crystallize as yellow prisms. Yield of **12a**: 0.438 g (91%). Anal. Calcd for $C_{30}H_{66}P_4Rh_2S_2$: C, 43.90; H, 8.11. Found: C, 43.82; H, 7.94. ^1H NMR (methylene chloride-d_2, −20 °C): δ 4.65 (t, J_{H-P} = 4.8 Hz, 1, H4), 1.82 (s, 3, H6's), 1.69 (dq, J = 7.8 Hz, 6, PEt_3 CH_2's), 1.60 (d, J_{H-P} = 6.0 Hz, 9, PMe_3), 1.35 (s, 3, H5's), 1.07 (dt, J_{H-P} = 13.8 Hz, J_{H-H} = 7.5 Hz, 9, PEt_3 CH_3's), 0.95 (br m, partially obscured, 1, H1), 0.75 (br m, partially obscured, 1, H1). $^{13}C\{^1H\}$ NMR (methylene chloride-d_2, −20 °C): δ 140.0 (s, C2 or C3), 137.4 (d, J_{C-P} = 15.2 Hz, C2 or C3), 79.3 (br d, J_{C-P} =

Table 2. X-ray Diffraction Structure Summary for 9, 10a, 11b, 12a, and 13a

	9	10a	11b	12a	13a
empirical formula	$C_{36}H_{78}P_4Rh_2S_2$	$C_{22}H_{47}OP_2RhS$[a]	$C_{12}H_{27}P_2RhS$	$C_{16}H_{35}Cl_2P_2RhS$[b]	$C_{34}H_{66}N_2P_2Rh_2S_2$
fw	904.80	524.51	368.25	495.25	834.77
cryst syst	triclinic	triclinic	orthorhombic	monoclinic	monoclinic
space group	$P\bar{1}$	$P\bar{1}$	*Fdd*2	$P2_1/n$	$P2_1/n$
a, Å	11.6559(2)	10.5114(3)	22.3840(6)	10.41510(10)	12.2598(5)
b, Å	12.6042(2)	12.0136(4)	31.1065(9)	19.0763(3)	12.0053(4)
c, Å	17.2786(3)	12.8913(4)	9.4465(3)	11.4420(2)	13.5413(5)
α, deg	89.4280(10)	98.311(1)	90	90	90
β, deg	72.8430(10)	110.247(1)	90	96.8390(10)	90.583(2)
γ, deg	69.0210(10)	115.310(1)	90	90	90
V, Å^3	2251.67(7)	1296.01(7)	6577.5(3)	2257.14(6)	1992.94(13)
Z	2	2	16	4	2
cryst dimens, mm	0.27 × 0.19 × 0.18	0.28 × 0.22 × 0.20	0.25 × 0.08 × 0.05	0.28 × 0.24 × 0.24	0.19 × 0.17 × 0.10
calcd density, g/cm^3	1.335	1.344	1.487	1.457	1.391
radiation; *λ*, Å	0.710 73	0.710 73	0.710 73	0.710 73	0.710 73
temp, K	165(2)	170(2)	165(2)	165(2)	100(2)
θ range, deg	1.74−29.00	1.79−28.00	2.24−27.50	2.09−29.00	2.23−35.49
data collected					
h	−15 to +15	−13 to +13	−28 to +28	−14 to +14	−17 to +20
k	−17 to +16	−15 to +15	−40 to +40	−26 to +25	−13 to +19
l	−23 to +23	−17 to +17	−12 to +12	−15 to +15	−18 to +22
total decay	none obsd	none obsd	none obsd	none obsd	none obsd
no. of data collected	47 530	26 059	20 235	46 030	79 728
no. of unique data	11 662	6200	3744	5996	9061
Mo Kα linear abs coeff, mm^{-1}	0.990	0.873	1.337	1.223	1.037
abs cor applied	empirical (SADABS)	empirical (SADABS)	empirical (SADABS)	empirical (SADABS)	empirical (SADABS)
data to param ratio	29.38	14.73	16.57	28.69	45.53
final *R* indices (obsd data)[c]					
R1	0.0573	0.0359	0.0273	0.0272	0.0275
wR2	0.0805	0.0678	0.0538	0.0561	0.0559
R indices (all data)					
R1	0.0763	0.0401	0.0345	0.0342	0.0383
wR2	0.0842	0.0690	0.0556	0.0583	0.0594
goodness of fit	1.229	1.257	1.046	1.059	1.033

[a] Includes 1 molecule of tetrahydrofuran. [b] Includes 1 molecule of methylene chloride. [c] $I > 2\sigma(I)$.

65.2 Hz, C4), 25.7 (br d, J_{C-P} = 21.1 Hz, C1), 20.1 (s, C5), 20.1 (s, C6), 19.3 (d, J_{C-P} = 16.5 Hz, PMe_3), 18.7 (d, J_{C-P} = 20.7 Hz, PEt_3 CH_2's), 8.4 (d, J_{C-P} = 3.0 Hz, PEt_3 CH_3's). $^{31}P\{^1H\}$ NMR (methylene chloride-d_2, 22 °C): δ 27.5 (dd, J_{P-Rh} = 166.0 Hz, J_{P-P} = 10.3 Hz, 1, PEt_3), −18.9 (dd, J_{P-Rh} = 120.9 Hz, J_{P-P} = 10.3 Hz, 1, PMe_3).

Synthesis of [S═CHC(Me)═C(Me)CH_2Rh(PEt_3)($CNCMe_3$)]$_2$ (13a). Compound **10a**, [S═CHC(Me)═C(Me)CH_2Rh(PEt_3)$_2$]$_2$ (0.074 g, 0.082 mmol), was dissolved in 10 mL of methylene chloride to form a yellowish brown solution and then cooled to −30 °C. *tert*-Butyl isocyanide (0.013 g, 0.164 mmol) was added to this solution at −30 °C via syringe. The resulting solution was warmed to room temperature and stirred for an additional 15 min, during which time the color changed from yellowish brown to dark orange. The volatiles were removed in vacuo, resulting in a dry yellowish orange film of compound **13a**. This residue was washed with cold pentane and redissolved in a minimal quantity of methylene chloride. When it was cooled to −30 °C, compound **13a** crystallized as off-white plates. Yield of **13a:** 0.055 g (81%). Anal. Calcd for $C_{34}H_{66}N_2P_2Rh_2S_2$: C, 48.92; H, 7.97. Found: C, 48.75; H, 7.57. ^1H NMR (methylene chloride-d_2, −20 °C): δ 4.45 (d, J_{H-P} = 4.2 Hz, 1, H4), 1.73 (s, 3, H6's), 1.60 (dq, *J* = 7.2 Hz, 6, PEt_3 CH_2's), 1.56 (s, 9, isocyanide Me's), 1.27 (s, 3, H5's), 1.15 (m, 1, H1), 1.04 (dt, J_{H-P} = 14.4 Hz, J_{H-H} = 7.2 Hz, 9, PEt_3 CH_3's), 0.75 (dd, *J* = 14.4 Hz, 7.2 Hz, 1, H1). $^{13}C\{^1H\}$ NMR (methylene chloride-d_2, −20 °C): δ 153.9 (d, *J* = 52.5 Hz, *C*$NCMe_3$), 139.2 (s, C2 or C3), 136.3 (s, C2 or C3), 76.6 (dd, *J* = 14.0 Hz, 5.1 Hz, C4), 55.7 (s, CN*C*Me_3), 31.1 (s, CNC(*C*H_3)$_3$), 23.9 (dd, *J* = 20.5 Hz, 6.3 Hz, C1), 19.9 (s's, C5 and C6), 17.5 (d, J_{C-P} = 21.7 Hz, PEt_3 CH_2's), 7.9 (s, PEt_3 CH_3's). $^{31}P\{^1H\}$ NMR (methylene chloride-d_2, 22 °C): δ 32.3 (d, J_{P-Rh} = 163.3 Hz, PEt_3).

General Comments on X-ray Diffraction Studies. Single crystals of Compounds **1**−**4**, **7**, **9**, **10a**, **11b**, **12a**, and **13a** were mounted on glass fibers under a nitrogen atmosphere. X-ray data were collected on a Bruker SMART or a Bruker Kappa Apex II charge coupled device (CCD) detector system at low temperature. Graphite-monochromated Mo Kα radiation was supplied by a sealed-tube X-ray source.

Structure solution and refinement were carried out using the SHELXTL-PLUS software package (PC version).[23] The rhodium atom positions were determined by direct methods. The remaining non-hydrogen atoms were found by successive full-matrix least-squares refinement and difference Fourier map calculations. In general, non-hydrogen atoms were refined anisotropically, while hydrogen atoms were either refined isotropically or were placed at idealized positions and assumed the riding model. Structural disorders in compounds **1**, **3**, **4**, **7**, **10a**, **12a**, and **13a** were treated and resolved as described below.

In the case of **1**, the solvent molecule, toluene, exhibited a commonly observed disorder due to a forced crystallographic inversion center. The complete molecule, including the symmetry-generated part, was refined with an occupancy of 50% and the same anisotropic displacement parameters (EADP) for all of the atoms.

Compound **3** crystallized with two independent molecules in the unit cell. In one of these molecules, the sulfur atom was disordered over two positions linked to C1 and C4, making these two carbons equivalent. The sulfur atom positions were assigned occupancy factors of 80% and 20% and refined anisotropically. A projection view of the disordered molecule is included in the Supporting Information.

(23) Sheldrick, G. M. SHELXTL-PLUS; Bruker Analytical X-ray Division, Madison, WI, 2005.

In compound **4**, rotational disorders were observed for the BF_4 anion and one of the solvent CH_2Cl_2 molecules. The BF_4 disorder was resolved with the location of two positions for every F atom (50% occupancies), and the two sets were refined independently with anisotropic thermal parameters. In the CH_2Cl_2 solvent molecule, one Cl atom displayed a 2-fold disorder, and the two positions were refined anisotropically with occupancies of 75% and 25%.

Compound **7** exhibited multiple disorders. First, the PMe_3 ligands showed positional disorder, and these disordered methyl groups were all modeled with 50% occupancies. The P−C distances for the disordered methyls were refined with SADI restraints. Second, the sulfur atom was disordered over two positions linked to C1 and C4, making these carbons equivalent (as in compound **3**). Both sulfur positions were refined anisotropically with 50% occupancies. This sulfur disorder allowed the bridging methylene carbon (C7) to serve as a crystallographic inversion center. A projection view of the molecule showing these disorders is included in the Supporting Information.

In compound **10a**, one of the methyl groups in a PEt_3 ligand exhibited a simple 2-fold disorder. Both carbon positions were refined anisotropically using 50% occupancies. In **12a**, the CH_2Cl_2 solvent molecule displayed a simple 2-fold disorder of one Cl atom. These two positions were refined anisotropically with partial occupancies of 72% and 28%. Finally, in **13a** one of the methyl groups in the *tert*-butyl isocyanide ligand exhibited a 2-fold disorder. Both atom positions were refined anisotropically with occupancies of 50%.

The structure of compound **4** included a large residual peak (2.784 e/Å^3) and hole (−1.4344 e/Å^3) at distances of 0.85 and 0.79 Å, respectively, from the rhodium atom. Due to the large amount of CH_2Cl_2 solvent in the crystals (four molecules of CH_2Cl_2 per molecule of **4**), they rapidly redissolved, even at low temperature. Therefore, we were unable to do careful crystal screening or shaping and were forced to collect data on irregularly faceted crystals. Attempts to treat the data with both empirical and face-indexed absorption corrections did not result in significant improvement in the residual peak intensities.

Crystal data and details of both collection and structure analysis are given in Tables 1 and 2.

Acknowledgment. Support from the National Science Foundation and the donors of the Petroleum Research Fund, administered by the American Chemical Society, is gratefully acknowledged. We also thank Pfizer Global Research and Development for a Summer Undergraduate Research Fellowship and Washington University for a Hoopes Undergraduate Research Fellowship to E.S.W. Washington University's High Resolution NMR Service Facility was funded in part by NIH Support Instrument Grants (Nos. RR-02004, RR-05018, and RR-07155). The regional X-ray Facility at the University of Missouri—St. Louis was funded in part by the National Science Foundation's MRI Program (Grant No. CHE-0420497).

Supporting Information Available: Listings of final atomic coordinates, thermal parameters, bond lengths, and bond angles for compounds **1**−**4**, **7**, **9**, **10a**, **11b**, **12a** and **13a**. This material is available free of charge via the Internet at http://pubs.acs.org.

OM058058F